BioMed Research International

Biomedical Studies of Ancient Asian Humans and Animals

Lead Guest Editor: Dong H. Shin
Guest Editors: Hisashi Fujita and Yi-Suk Kim

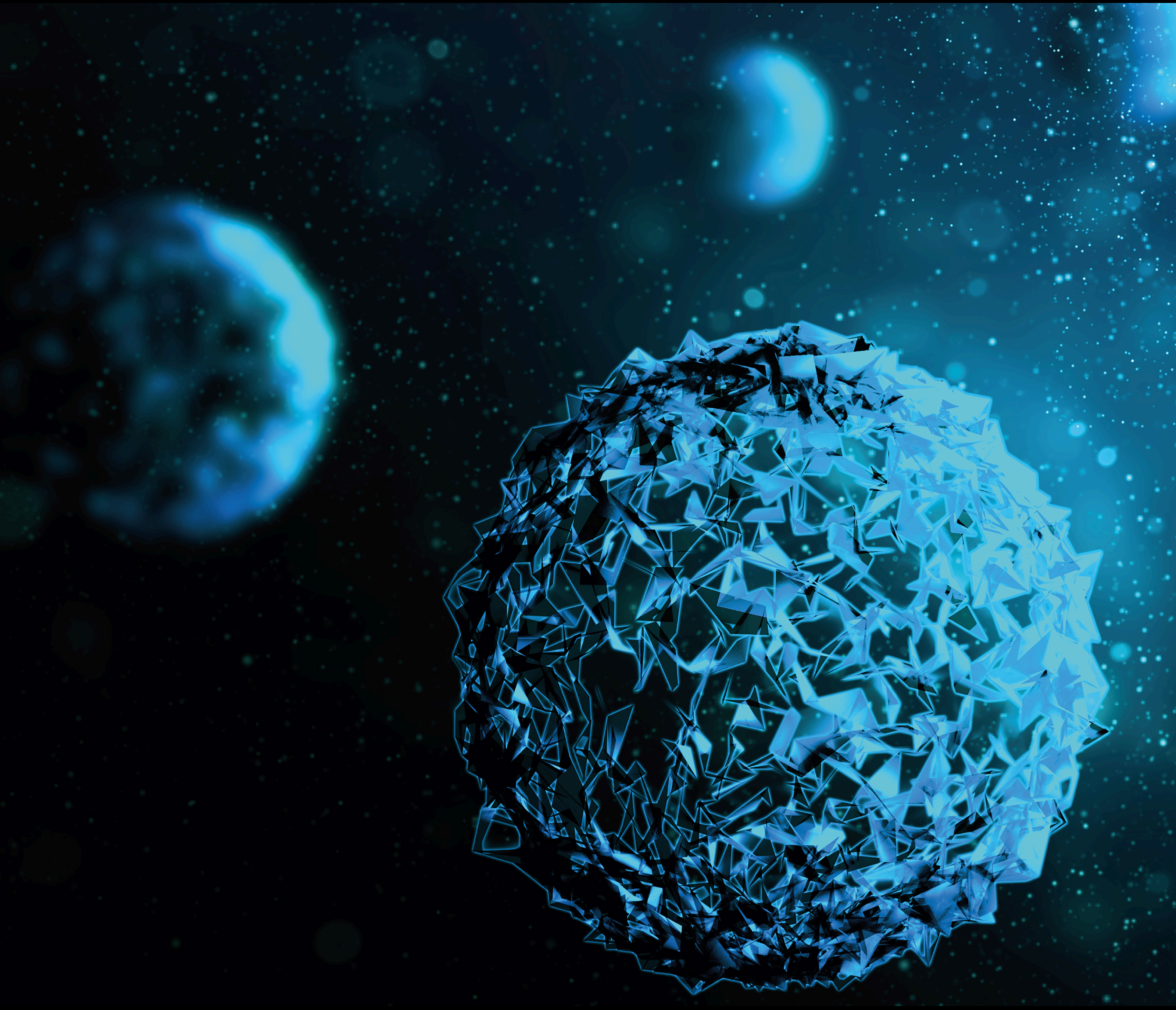

Biomedical Studies of Ancient Asian Humans and Animals

BioMed Research International

Biomedical Studies of Ancient Asian Humans and Animals

Lead Guest Editor: Dong H. Shin
Guest Editors: Hisashi Fujita and Yi-Suk Kim

Section Editors

Academic Editors

Bioinformatics

Contents

Hindawi
BioMed Research International
Volume 2022, Article ID 2069063, 14 pages
https://doi.org/10.1155/2022/2069063

Research Article

Application of Methods for a Morphological Analysis of the Femoral Diaphysis Based on Clinical CT Images to Prehistoric Human Bone: Comparison of Modern Japanese and Jomon Populations from Hegi Cave, Oita, Japan

Daisuke Endo,[1] **Kazunobu Saiki**,[1] **Minoru Yoneda**,[2] **Hajime Ishida**,[3] **Keiko Ogami-Takamura**,[1,4,5] **Rina Sakai**,[6] **Kiyohito Murai**,[1] **Takeshi Imamura**,[1] **Yoshiatsu Naito**,[7] **Tetsuaki Wakebe**,[1,8] **and Toshiyuki Tsurumoto**[1,4]

[1]*Department of Macroscopic Anatomy, Graduate School of Biomedical Sciences, Nagasaki University, 1-12-4 Sakamoto, Nagasaki, Nagasaki 852-8523, Japan*
[2]*The University Museum, The University of Tokyo, 7-3-1 Hongo, Bunkyo-ku, Tokyo 113-0033, Japan*
[3]*Department of Human Biology and Anatomy, Graduate School of Medicine, University of the Ryukyus, Senbaru 1, Nishihara, Okinawa 903-0213, Japan*
[4]*Center of Cadaver Surgical Training, School of Medicine, Nagasaki University, 1-12-4 Sakamoto, Nagasaki, Nagasaki 852-8523, Japan*
[5]*Department of Anesthesiology and Intensive Care Medicine, Graduate School of Biomedical Sciences, Nagasaki University, 1-7-1 Sakamoto, Nagasaki, Nagasaki 852-8501, Japan*
[6]*School of Medicine, Nagasaki University, 1-12-4 Sakamoto, Nagasaki, Nagasaki 852-8523, Japan*
[7]*Nagasaki University, 1-12-4 Sakamoto, Nagasaki, Nagasaki 852-8523, Japan*
[8]*Nagasaki Medical College, 36-59 Atago, Nagasaki, Nagasaki 850-0822, Japan*

Correspondence should be addressed to Daisuke Endo; leopard72endu@gmail.com

Received 22 November 2021; Revised 26 April 2022; Accepted 4 May 2022; Published 7 June 2022

Academic Editor: Hisashi Fujita

A morphological analysis of ancient human bones is essential for understanding life history, medical history, and genetic characteristics. In addition to external measurements, a three-dimensional structural analysis using CT will provide more detailed information. The present study examined adult male human skeletons excavated from Hegi cave, Nakatsu city, Oita Prefecture. CT images were taken from the femurs of adult males (Initial/Early Jomon Period ($n = 10$) and Late Jomon Period ($n = 5$)). Cross-sectional images of the diaphysis from below the lesser trochanter to above the adductor tubercle were obtained using the method established by Imamura et al. (2019) and Imamura et al. (2021). Using Excel formulas and macros, the area of cortical bone, thickness, and degree of curvature were quantitatively analyzed. The results were compared with data on modern Japanese. The maximum thickness of cortical bone in the diaphysis and the degree of the anterior curvature were significantly greater in Late Jomon humans than in the other groups. In contrast to modern humans, the majority of Jomon femurs showed the S-shaped curvature with the medial side at the top position and the lateral side at the lower position. The present results demonstrate that Late Jomon humans had a wider range of activity than the other groups and also provide insights into diseases in the hip and knee joints of Jomon humans.

1. Introduction

A morphological analysis of bone provides various types of information, such as the risk of fracture. Relationships have been reported between the angle between the femoral head and diaphysis [1], the increased curvature of the diaphysis, and atypical fractures in the femur [2–4]. Furthermore, as the lateral curvature of the femur increases, fracture sites have been shown to move from below the subtrochanteric region to the midportion of the diaphysis [5, 6]. On the other hand, the removal of cancellous bone from the femoral neck did not significantly change the strength of the femur [7], suggesting that cortical bone defines the strength of the femur. The risk of femoral fracture is higher in women, and even after standardization for body size, the femoral diaphysis is still thinner in women than in men and possesses less cortical bone [8]. Therefore, the morphology of cortical bone in the femoral diaphysis may be important for predicting the risk of fracture; however, a simple and reproducible method for its assessment has not yet been established. Although the increased curvature of the diaphysis has been implicated as a risk factor for atypical fractures, there is currently no unified method for a quantitative analysis of anterior and lateral curvatures with high reproducibility. Therefore, we developed methods to quantitatively analyze the morphology of cortical bone using CT images of modern Japanese skeletal specimens, with a threshold value that distinguishes cortical bone from cancellous bone [9, 10]. This method may become the standard for a morphological analysis because it is completed in Excel and does not require specific software. Using this method, it is possible to obtain quantitative values for the periosteal border length (PBL), the area of cortical bone in a cross-section, cortical bone occupancy (cortical index (CI)) relative to the total area of the cross-section, cortical bone thickness, and the degrees of the anterior and lateral curvatures of the diaphysis relative to the bone axis. This analysis revealed marked diversity in the morphology of cortical bone and also showed that the area of cortical bone, CI, and cortical bone thickness were affected by sex and age. We previously demonstrated that bone morphology correlated with mechanical functions by comparing these quantitative values to the findings of a finite element analysis using a 3D model constructed from CT images [11]. In addition to the estimation of disease risk, bone morphology has been considered to reflect the living environment of adults [12–14] based on Wolff's law that bone morphology changes to adapt to a given load [15]. Therefore, differences in the curvature of the femoral diaphysis among populations and differences in femoral morphology among various groups of archaic human bones have been analyzed to investigate the living environment [16, 17]. Novel insights are anticipated with the application of the methods already established for a morphological analysis to archaic human bones. Therefore, the present study examined femurs excavated from Hegi cave. Sixty-seven ancient human bones have been excavated from Hegi cave in Nakatsu city, Oita Prefecture, Kyushu Island, Japan [18]. Fifteen male femurs with well-preserved diaphyses were selected for analyses. There are two reasons why we chose males. The first is that we were able to analyze a statistically processable number of male femurs from different periods of the Jomon period. The other reason is that the age at death of human bones excavated from the Hegi cave cannot be strictly estimated, and the bones used for analysis can only be said to be those of adults. The results of the analysis by Imamura et al. showed that age had a smaller effect on morphological parameters in males than in females, and no significant correlation has been found [9]. Therefore, the influence of age was considered small in comparison with modern humans. These bones were dated using the ^{14}C method established by Yoneda et al. [19] and divided into two groups: those belonging to the Initial/Early Jomon Period and to the Late Jomon Period. We compared measurements in each group with those of modern humans [7, 8]. The Late Holocene is dated to the Late Jomon Period, while the other groups are roughly dated to the Initial/Early Jomon Period. In the Holocene, which began with the end of the Ice Age, the Late Holocene is the period during which temperatures dropped and many settlements disappeared [20, 21]. Changes in the living environment may be reflected not only by comparisons between modern humans and the prehistoric remains excavated from Hegi cave but also differences in the ages of the prehistoric remains.

2. Materials and Methods

Human femurs were excavated from Hegi cave in Nakatsu city, Oita Prefecture, Japan (Figure 1). The skeletal remains from the cave have been legally preserved in the Department of Macroscopic Anatomy, Graduate School of Biomedical Sciences, Nagasaki University, which was involved in the excavation project [18].

2.1. Radiocarbon Dating of Samples. The methods used to date the bones analyzed were previously reported by Yoneda et al. [19]. In brief, gelatine from biogenic collagen was extracted from bones. For the ^{14}C analysis, 1.2–2.5 mg of collagen, containing approximately 0.5–1 mg of carbon, was oxidized to CO_2 in evacuated tubes with copper dioxide at a temperature of 850°C, and CO_2 was then cryogenically purified in a vacuum system [22]. The radiocarbon content of the mixture of graphite and iron powder was measured using accelerator mass spectrometry (AMS) at The University of Tokyo [23]. Fifteen femurs were divided into the Initial/Early Jomon ($n = 10$, ca. 10,200-6,500 cal BP) and Late Jomon ($n = 5$, ca. 4,500-4,000 cal BP) groups based on the results of radiocarbon dating (Table 1 and Figure 2).

2.2. Assessment of Age and Sex. The age and sex of the Jomon paleo-human remains analyzed were established based on the morphological features of the skull and pelvic bone and reported in Chapter 6 of the Honyabakei Town History [18]. Fifteen male femurs in good condition were selected from 67 archaeological remains. The ages of the owners of those femurs were all estimated to be adults over 20 years old.

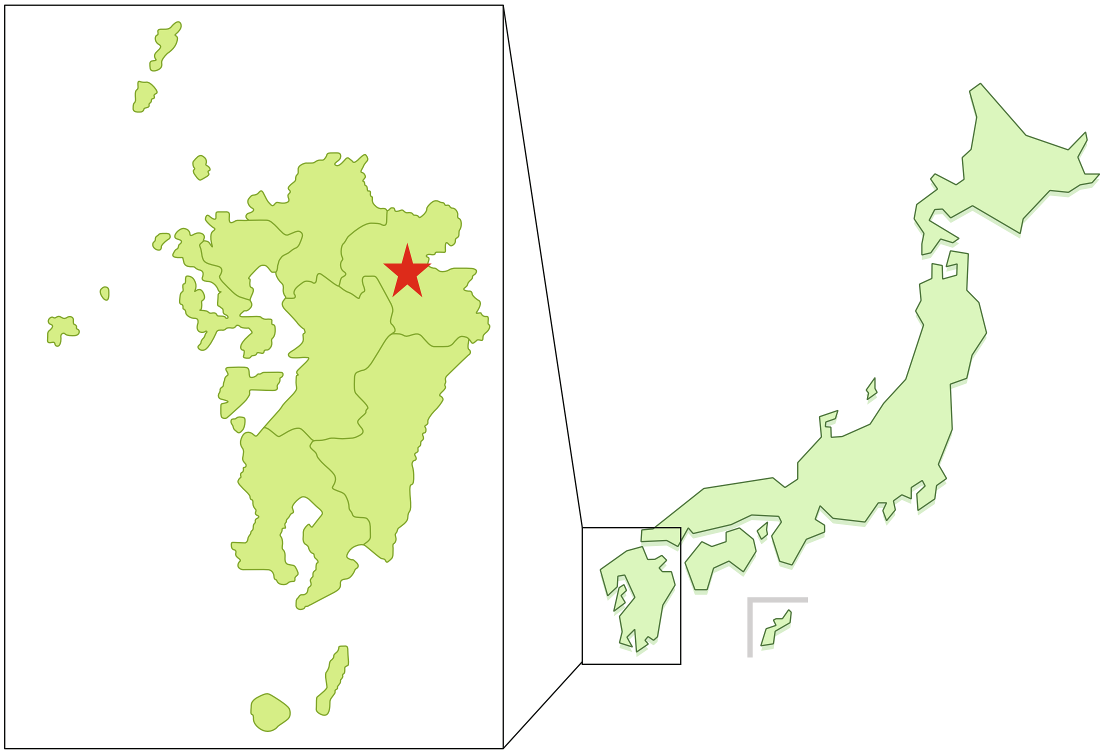

Figure 1: Location of Hegi cave in Nakatsu city, Oita Prefecture, Japan.

2.3. CT Imaging and Extraction of Target Images. Full-length images of all examined femurs were obtained using clinical multislice CT (Activision 16, Toshiba Corp., Tokyo, Japan) (X – tube volume/current = 120 kV/100 mA, image matrix size: 512 × 512 pixels, and slice thickness: 0.5 mm) installed at the Graduate School of Biomedical Sciences, Nagasaki University. This slice thickness resulted in an error of up to 0.6% in morphological parameters. Since the plane resolutions of CT were assessed using a field size divided by 512, they were not constant and ranged between 0.158 and 0.292 mm (mean value, 0.213 mm). Bones were placed with the posterior side down and grounded on the table of the imaging device at three points: the most posterior points of the greater trochanter, medial condyle, and lateral condyle. Data were saved in the Digital Imaging and Communication in Medicine (DICOM) format. The range between the lower end of the lesser trochanter and adductor tubercle of each femur was divided into nine segments of equal lengths. Cross-sections, including both ends, were labeled from the top to bottom as "level 1" to "level 10" (Figure 3). Threshold values for the definition of the cortex were calculated as described in our previous study [9] and assessed as follows: (i) all of the matrixes for the ten levels were pasted into one Microsoft Excel sheet, and (ii) a histogram was created based on a frequency table of Hounsfield units (CT values) to calculate the mean CT value for the first peak (i.e., approximately -1000; mainly indicating the CT value of the surrounding air) and the CT value for the second peak (i.e., indicating the CT value of the bone itself).

2.4. Quantification of Morphological Elements of the Femoral Diaphysis Using an Image Analysis. The methods used to quantify the morphological parameters of cross-sections of the femoral diaphysis using CT data were previously reported by Imamura et al. [9]. All calculations were conducted using Microsoft Excel. In brief, cross-sectional areas were calculated by counting all points surrounded by the periosteal perimeter. Regarding the area of cortical bone, all points surrounded by both the periosteal and endosteal perimeters of cortical bone were counted. This area was corrected by calculating the actual length per pixel in DICOM data to consider the magnification ratio at the time of imaging. The ratio of the area of cortical bone to the cross-sectional area was calculated as the cortical index (CI). PBL in each section was calculated by counting the number of all points on the periosteal surface. To evaluate cortical bone thickness, distances between a point on the periosteal surface and all points on the endosteal surface of cortical bone were calculated. The minimum of these values was defined as the cortical bone thickness of the point. Calculations were performed for all points of the periosteal surface of cortical bone. The maximum and mean values of all points were defined as maximum and mean cortical bone thicknesses, respectively. The measurement results were represented without and with standardization by dividing by the total length of each femur.

2.5. Quantification of the Degree of Curvature by an Image Analysis. The method used to quantify the degree of curvature was reported by Imamura et al. [10]. The central mass distribution (CMD) of cross-sectional images was assessed as the intersection of two line segments dividing any two-dimensional figure into equal areas. The CMD curve was obtained by connecting all CMDs of the nine cross-sections of the femur. Shifts in the x- and y-axis directions

Table 1: Conventional (years before present, BP) and calibrated radiocarbon ages (calibrated years before present, cal BP) of the femurs excavated from Hegi cave.

No.	Period	Conventional ^{14}C age (BP)	AMS lab ID	Calibrated ^{14}C age (cal BP) 68.3%	Calibrated ^{14}C age (cal BP) 95.4%
1	Late Jomon	3928 ± 28	TKA-18741	4419 (46.0%) 4352 4329 (22.3%) 4298	4507 (2.2%)4490 4438 (88.2%) 4286 4275 (5.1%) 4248
2	Late Jomon	3757 ± 23	PLD-19678	4217 (3.3%) 4211 4153 (65.0%) 4086	4231 (10.8%) 4200 4180 (1.4%) 4169 4159 (70.0%) 4077 4039 (13.2%) 3992
3	Late Jomon	3807 ± 23	PLD-19679	4236 (36.6%) 4194 4188 (31.6%) 4152	4289 (3.4%) 4268 4255 (81.4%) 4142 4126 (10.6%) 4093
4	Late Jomon	3913 ± 29	TKA-18742	4414 (43.8%) 4350 4331 (24.4%) 4296	4420 (95.4%) 4245
6	Late Jomon	3890 ± 23	PLD-19680	4405 (39.7%) 4345 4338 (28.5%) 4293	4411 (95.4%) 4246
16	Early Jomon	5925 ± 25	PLD-18261	6787 (53.0%) 6730 6698 (15.2%) 6679	6830 (1.9%) 6820 6796 (93.6%) 6669
19	Early Jomon	6285 ± 31	TKA-18746	7256 (55.6%) 7192 7180 (12.6%) 7166	7280 (95.0%) 7156 7091 (0.4%) 7082
29	Early Jomon	6286 ± 33	TKA-18753	7256 (22.7%) 7231 7225 (31.1%) 7190 7183 (14.5%) 7166	7307 (1.0%) 7291 7285 (94.0%) 7156 7091 (0.5%) 7082
35	Early Jomon	6667 ± 33	TKA-18757	7578 (22.5%) 7557 7545 (45.7%) 7508	7603 (0.4%) 7600 7593 (93.4%) 7472 7443 (1.6%) 7434
39	Early Jomon	6524 ± 32	TKA-18760	7480 (56.8%) 7421 7380 (11.5%) 7361	7556 (1.6%) 7547 7508 (69.2%) 7418 7390 (24.7%) 7331
40	Early Jomon	6382 ± 31	TKA-18761	7411 (6.4%) 7402 7325 (61.9%) 7264	7421 (17.7%) 7381 7359 (73.6%) 7255 7197 (4.1%) 7177
46	Early Jomon	5864 ± 39	TKA-18766	6738 (68.3%) 6648	6786 (90.3%) 6600 6590 (5.1%) 6561
56	Initial Jomon	8926 ± 30	PLD-18263	10183 (31.3%) 10120 10064 (13.4%) 10037 10028 (7.4%) 10010 9991 (16.2%) 9960	10193 (35.2%) 10110 10080 (60.3%) 9909
59	Initial Jomon	8564 ± 51	MTC-15609	9550 (68.3%) 9488	9664 (3.1%) 9640 9631 (92.4%) 9470
60	Early Jomon	6514 ± 39	TKA-18770	7473 (21.1%) 7444 7434 (14.2%) 7420 7383 (33.0%) 7335	7554 (0.8%) 7549 7507 (51.6%) 7412 7402 (43.0%) 7325

of CMD at each level from the line connecting the CMDs of the first and ninth cross-sections were calculated.

2.6. Statistical Analysis. The goodness-of-fit test was performed to confirm the standard distribution of each parameter. A repeated measures two-factor ANOVA followed by multiple comparisons with Scheffé's test was conducted to examine differences in morphological parameters among the modern, Initial/Early Jomon, and Late Jomon populations. A principal component analysis was performed using the mean value of each morphological element. Regarding the lateral curvature, we investigated whether the distribution of each curvature pattern differed among the modern, Initial/Early Jomon, and Late Jomon populations using the chi-squared independence test. Statistical analyses were conducted with Excel-based formulas and macros.

3. Results

3.1. A New Analysis Method Based on CT Images Revealed Differences in the Femoral Diaphysis between Modern and Jomon Humans. Mean and maximum cortical bone thicknesses, PBL, the area of cortical bone, the total cross-sectional area, and CI were measured in 8 cross-sections of

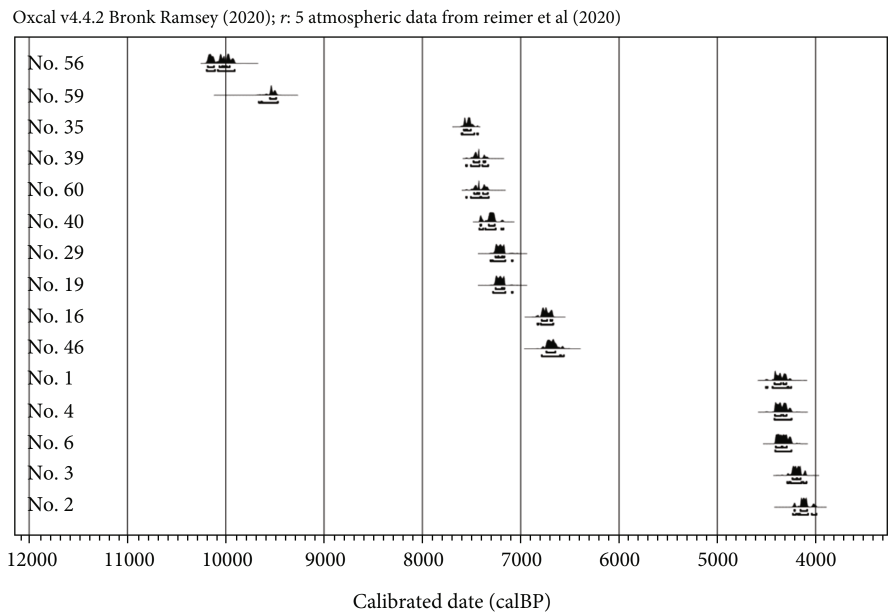

FIGURE 2: Probability distributions of calibrated ^{14}C dates of the femurs excavated from Hegi cave.

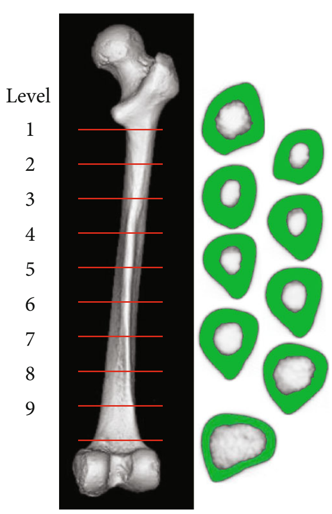

mean CBT (mm)	PBL (mm)	ACB (mm^2)
4.8	98.3	307.6
5.7	88.0	304.6
6.0	86.0	304.5
6.0	88.4	304.5
5.8	90.8	303.4
5.6	92.0	303.5
5.3	95.8	299.9
4.3	115.0	284.9
3.2	111.0	268.2

FIGURE 3: Example of results from the Late Jomon Period population. The shapes of cross-sections at eight levels are shown. In the table, the values for mean cortical bone thickness (mean CBT), periosteal border length (PBL), and the area of cortical bone (ACB) are shown. The image was composed with CT images using Radiant DICOM viewer (ver 2020 1.1 (64-bit), Mexidant, Poznan, Poland).

the femoral diaphysis (Figure 4). The mean, maximum, and CI of cortical bone thickness were higher at all levels in the order of the Late Jomon, Initial/Early Jomon, and modern populations. On the other hand, PBL and the total cross-sectional area were higher in the order of the modern, Initial/Early Jomon, and Late Jomon populations. Similar results were obtained when measurements were standardized by the length of the femoral diaphysis to exclude the effect of height (Figure 5). A two-way analysis of variance showed more combinations of significant differences after standardization, particularly for maximum cortical bone thickness, not only between the Jomon and modern populations but also between the Initial/Early and Late Jomon populations. A principal component analysis was performed using the mean values at all levels for the five morphological factors standardized by femoral diaphyseal length and CI. Eigenvectors obtained for the first and second principal component scores are shown in Table 2. The eigenvector for the first principal component was positive, except for CI, which was considered to reflect the size of the cross-section because the contributions of the cross-sectional area and perimeter diameter were large. On the other hand, CI and cortical bone thickness contributed positively, while the cross-sectional area and PBL contributed negatively to second principal component scores, reflecting the size of cortical bone. A scatter plot with the first principal component score on the x-axis and the second principal component score on the y-axis showed groups of bones in the order of the modern, Initial/Early Jomon, and Late Jomon populations (Figure 6).

3.2. The Degree and Pattern of Curvature Differs between Modern and Jomon Humans. The curvature of Jomon femurs excavated from Hegi cave was quantified using the method established by Imamura et al. [10]. All of the Jomon femurs were flexed anteriorly, and in comparisons with modern bones, the degree of curvature of Initial/Early Jomon bones was similar to that of modern bones, while Late Jomon bones showed significantly stronger curvature than modern and Initial/Early Jomon bones (Figure 7). While the anterior curvature of both Jomon and modern bones showed a primary curve with the apex in the middle of the femoral diaphysis, the lateral curvature showed a more diverse pattern (Figure 8). The majority of modern bones showed a lateral primary curve with the apex at the top of the femur diaphysis. Some of the modern and Jomon

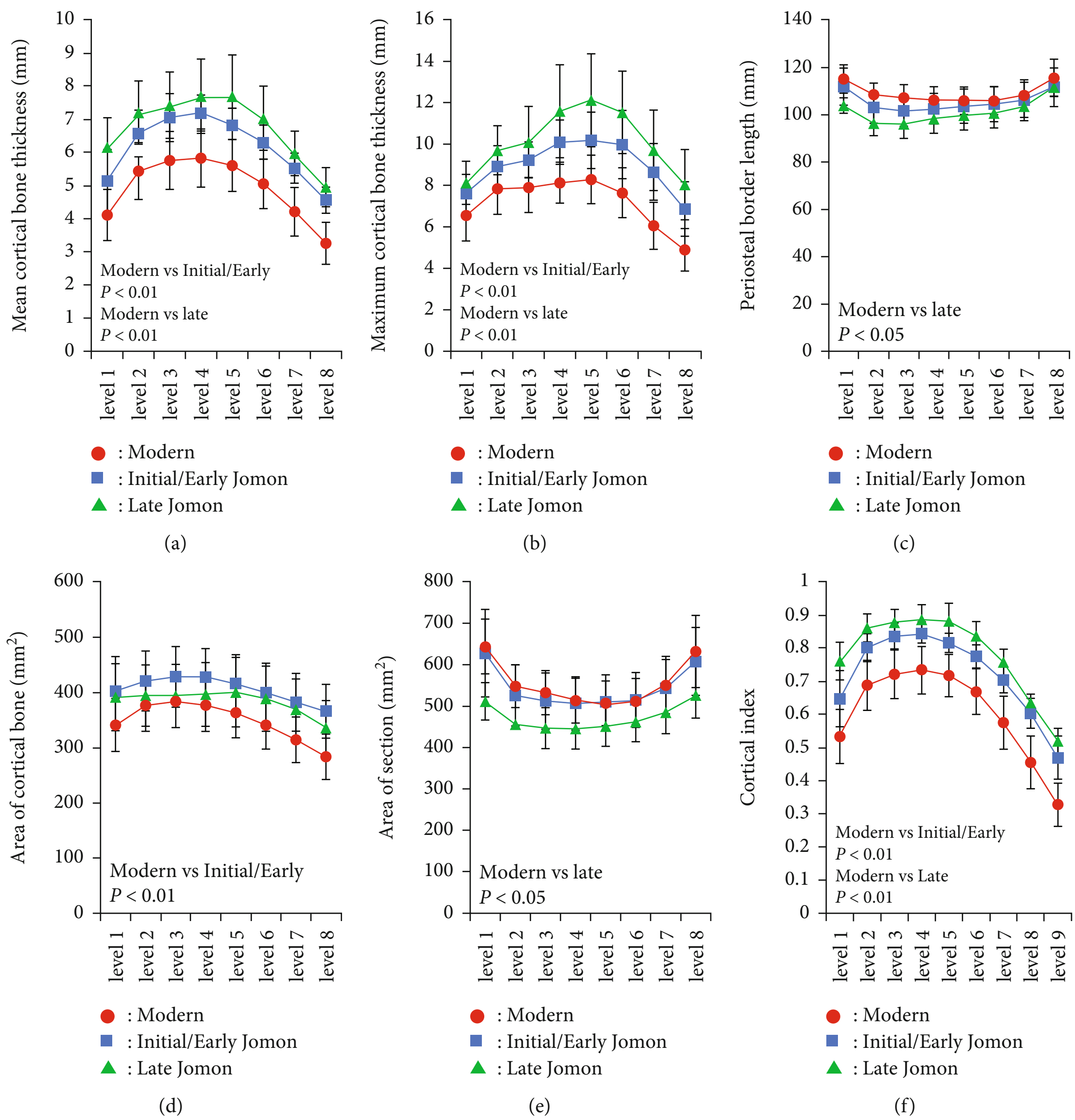

Figure 4: Morphological parameters of modern (Imamura, et al., [9]), Initial/Early Jomon, and Late Jomon Period populations. (a) Mean cortical bone thickness, (b) maximum cortical bone thickness, (c) periosteal border length, (d) area of cortical bone, (e) area of sections, and (f) cortical index. Averages are plotted at each cross-sectional level. Error bars indicate ±1 standard deviation. Significant differences analyzed by a two-way ANOVA followed by multiple comparisons were indicated in each graph.

bones also showed a primary curve of the medial curvature with an apex at the top of the diaphysis. On the other hand, many femurs had cross-sections with both medial and lateral center points relative to the bone axis connecting the center points of levels 1 and 9. In contrast to previous findings on modern bones, which all showed the lateral curvature at the top of the diaphysis and the medial curvature at the bottom, most of the Jomon bones showed the medial curvature at the top and the lateral curvature at the bottom, and the distribution of curvature patterns significantly differed among the groups (Table 3). Figure 9 shows a graph with mean curvature values at each level. Mean values and standard errors were used because some bones showed different kyphotic patterns. In contrast to the modern human skeleton, which has the lateral curvature at the top of the diaphysis, the Jomon human skeleton has the medial curvature at the top and the lateral curvature at the bottom, with the medial curvature at the top being more pronounced in the Initial/Early Jomon human and the lateral curvature at the bottom being more pronounced in the Late Jomon human.

4. Discussion

In the present study, we quantitatively analyzed the morphological features of cross-sections of the femoral diaphysis of Jomon humans excavated from Hegi cave based on CT images using an already established method for skeletal specimens of the modern Japanese population (Imamura et al., [9]; Imamura et al. [10]). Among the male femurs excavated, 15 with well-preserved diaphyses were selected for analysis. The acquisition of CT images, extraction of cross-sections at each level, the setting of thresholds for the

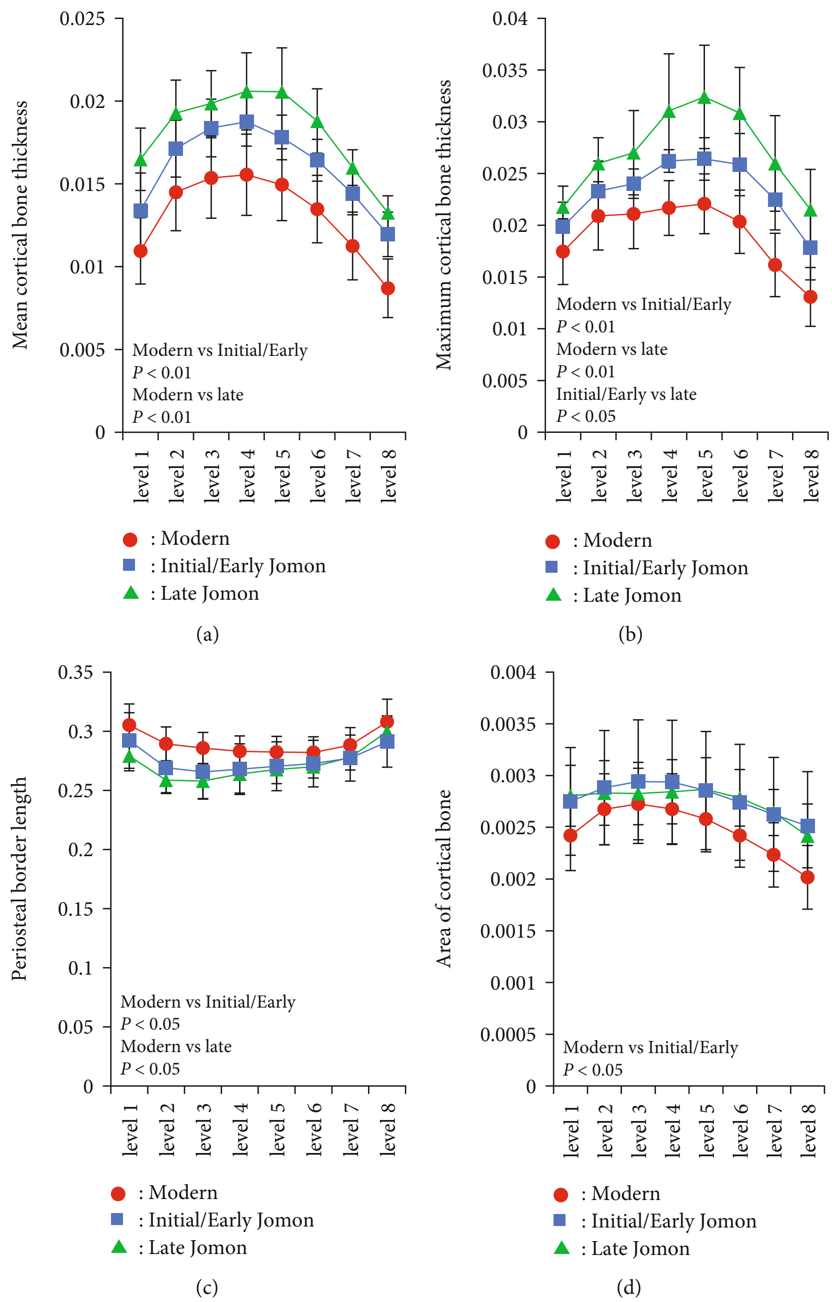

Figure 5: Continued.

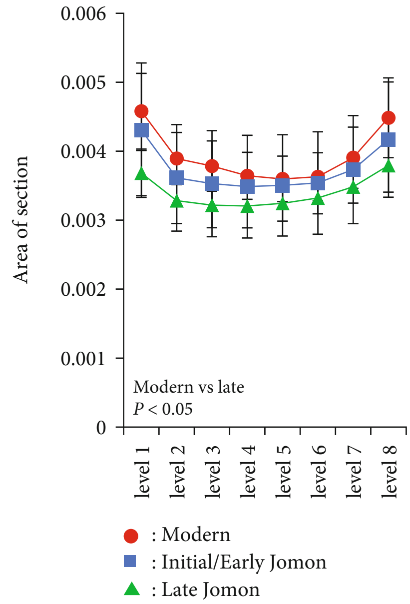

(e)

Figure 5: Morphological parameters standardized with diaphyseal lengths of modern (Imamura, et al.,[9]), Initial/Early Jomon, and Late Jomon Period populations. (a) Mean cortical bone thickness, (b) maximum cortical bone thickness, (c) periosteal border length, (d) area of cortical bone, and (e) area of section. Averages are plotted at each cross-sectional level. Error bars indicate ±1 standard deviation. Significant differences analyzed by a two-way ANOVA followed by multiple comparisons were indicated in each graph.

Table 2: Eigenvectors of a main component analysis with morphological parameters normalized with femoral lengths in modern, Initial/Early Jomon, and Late Jomon Period populations. These vectors were used to calculate the first and second principal component scores ($Z1$ and $Z2$), shown in Figure 6, respectively.

	$Z1$	$Z2$
Area of cortical bone	0.571	-0.003
Cross-sectional area	0.552	-0.202
Cortical index	-0.056	0.616
Periosteal border length	0.517	-0.133
Mean cortical bone thickness	0.292	0.544
Maximum cortical bone thickness	0.111	0.517

definition of cortical bone, and the acquisition of quantitative values were performed without any modifications from the protocol established for the modern Japanese population, indicating that the method is applicable to the measurement of archaic human bones and that the values obtained can be directly compared with those of the modern Japanese population. Femoral morphology is important not only for its clinical significance in predicting fracture risk [5–8] but also in terms of predicting the living environment [12–14]. However, as our previous studies have shown, the trends of age-related changes were different for diaphyseal peripheral border length and thickness of cortical bone. On the other hand, the thickness of cortical bone not peripheral border length was strongly correlated with the stress and strain applied to the femur with one-legged standing configuration estimated with the finite element method [11], suggesting that external measurement of femoral morphology alone is insufficient to estimate its function and that it is essential to analyze its internal structure. For this reason, many analyses have been performed using CT [24–26], but measurement conditions must be uniform to compare results among different populations. Various algorithms have been used to define cortical bone [27, 28], but no reproducible method has been established because it requires special software or programs and subjective judgment by the researcher. The method used in this study was completed on the highly generalized software Excel, and after CT images were acquired under the conditions described in this paper, the determination of threshold values to define cortical bone and the acquisition of analysis results could be performed mechanically, without requiring subjective judgment. No anomalous values that could be attributed to the method or results inconsistent with the impression received from the CT images were obtained during the analysis process. The fact that the method was applicable not only to modern bleached human bones but also to archaic femurs strongly suggests that the method can be applied to a very wide range of specimens.

Quantitative analysis of curvature was also possible by clearly separating anterior and lateral curvature. As discussed below, the anterior and lateral curvature is affected by different mechanical conditions, so this separation is essential to consider their background and significance. The degree of curvature of the diaphysis has been expected to be a distinguishing feature between different populations since Stewart's work in 1962 and has been studied not only about differences between Japanese and Ainu but also about behavior [17, 29, 30]. Since a unified method is still needed to facilitate such research, the importance of this method is

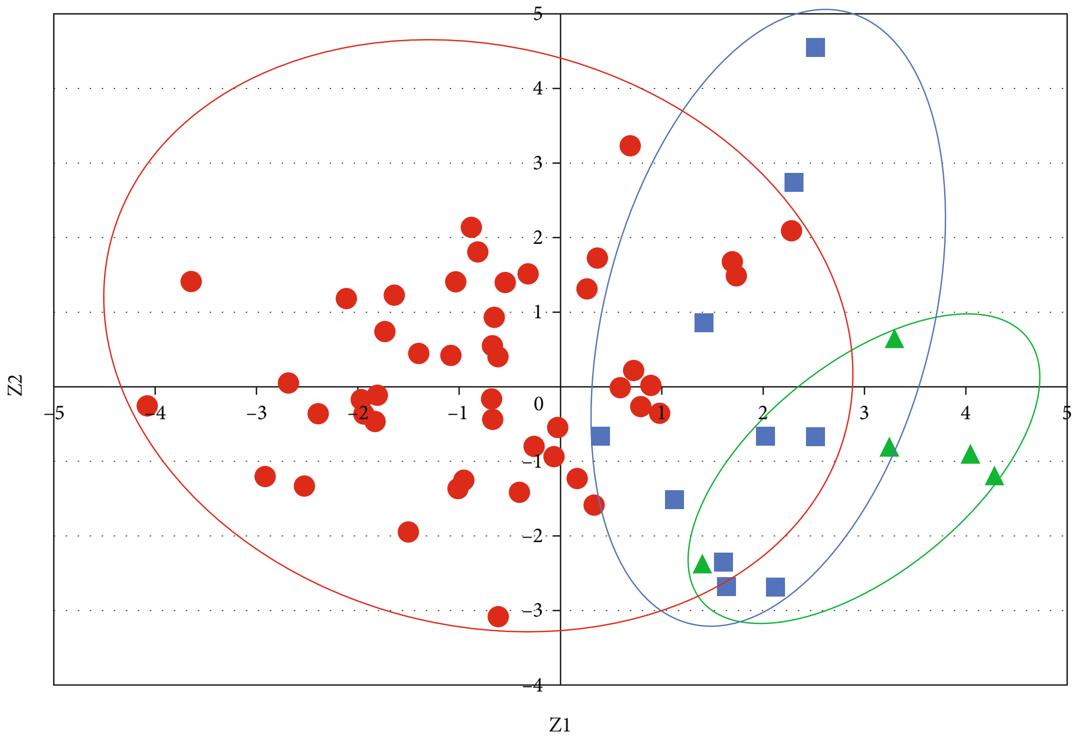

Figure 6: Principal component analysis of means of morphological parameters standardized with diaphyseal lengths. Red circles, blue squares, and green triangles indicate the principal component scores of modern, Initial/Early Jomon, and Late Jomon Period populations, respectively. Eigenvectors for each score, *Z*1 and *Z*2, are shown in Table 2.

very high. In the future, by estimating the results of biomechanical analysis from the multiple morphological data, it will be possible to compare femoral functions among different populations. Jomon Period femurs excavated from Hegi cave appeared to be thinner than modern femurs, while no significant differences were observed in femur lengths. This result was confirmed by a morphological analysis based on CT images. PBL of the diaphysis was the largest in modern femurs, and when standardized by the length of the diaphysis, modern femurs were significantly thicker than those from both the Initial/Early and Late Jomon Periods. In addition, the cross-sectional area of the modern femur was larger in than that in the Late Jomon femur, both before and after standardization. In contrast, the area of cortical bone and CI were significantly larger in Initial/Early Jomon femurs than in modern femurs before and after standardization, suggesting that in contrast to the apparent size of femurs, cortical bone may have been larger in Jomon humans. Imamura et al. reported that PBL, the area of cortical bone, and CI did not correlate with age in males, suggesting that the differences in morphological parameters among modern, Initial/Early Jomon, and Late Jomon humans do not reflect differences in the age of the human bones analyzed [9], even though the age of modern bones analyzed by Imamura et al. was biased towards older ages due to their sampling method; therefore, further studies are warranted. Mean cortical bone thickness in each cross-section was also larger in Initial/Early and Late Jomon femurs than in modern femurs, both before and after standardization by diaphyseal length. A previous study reported that the mean thickness of the diaphysis in modern skeletal specimens correlated with the stresses and strains applied to the diaphysis during a one-legged stance [11]. Furthermore, mean thickness values were high in Jomon humans, indicating that their femurs were highly resistant to force, particularly that applied along the bone axis. In previous studies on Jomon humans, PBL corrected by femur length was considered to represent the sturdiness of the femur [31]. This index increased from the middle Jomon Period, and the femur appeared to have become sturdier during this period [32]. In the present study, this index was lower in the Jomon Period, whereas the area and thickness of cortical bone were larger. These results strongly suggest that the femur was sturdier in the Jomon Period, particularly the Late Jomon Period; however, the mechanisms responsible were different.

Humans in the Jomon Period were found to have a more developed linea aspera than modern humans, which may reflect the genetic characteristics or living environment of Jomon humans. It is often expressed as the cross-sectional index, which is the ratio of the long to short diameter of the femoral diaphysis [33]. The index increased with age in Jomon humans and is significantly larger than that of modern humans, who show a smaller degree of increase after puberty, suggesting that it is strongly related to behavior for food gathering [34]. In the present study, instead of this ratio, we used CT to directly measure cortical bone thickness, which enabled us to remove the influence of medullary cavity morphology. The maximum thickness of cortical bone, which is considered to reflect the development of the linea aspera at the center of the diaphysis, was not only

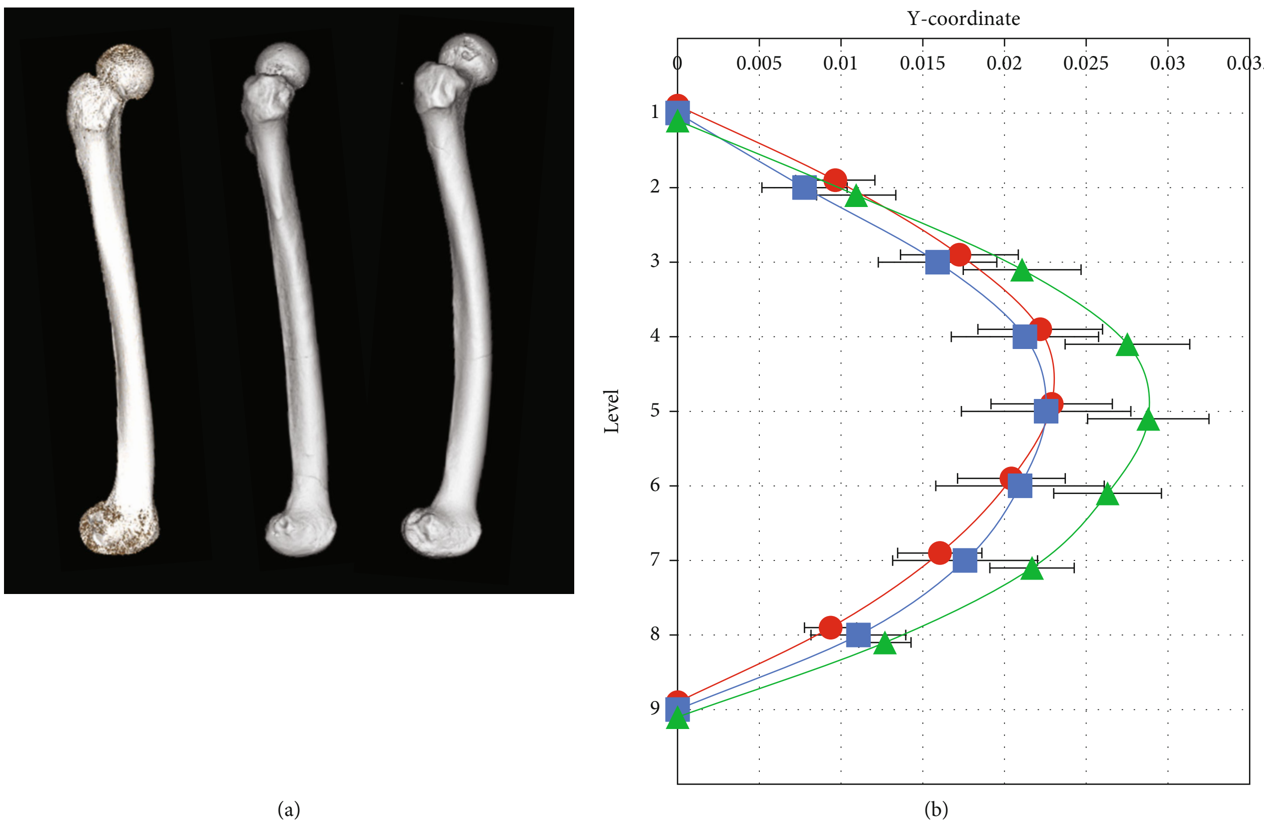

Figure 7: Comparison of the anterior curvature among modern, Initial/Early Jomon, and Late Jomon Period populations. (a) Examples of modern (left), Initial/Early Jomon (middle), and Late Jomon (right) Period populations. (b) Averaged degrees of the anterior curvature normalized with femoral lengths are shown. Circles represent the modern population, squares represent the Initial/Early Jomon Period population, and triangles represent the Late Jomon Period population. Averages are plotted at each cross-sectional level. Error bars indicate ±1 standard deviation. Significant differences were found between modern and Late Jomon Period populations ($p < 0.01$) and between the Initial/Early and Late Jomon Period populations ($p < 0.05$).

significantly different between modern and Jomon humans after standardization by the length of the diaphysis but was also significantly different between Initial/Early and Late Jomon humans. The linea aspera is an attachment site for the adductor muscle, and its degree of development is considered to reflect the extent of movement [35]. Since the linea aspera was significantly developed in femurs of Late Jomon humans, a wide range of movement appeared to be necessary for life in this time period. This is consistent with previous findings showing that the linea aspera of the femur of an Initial Jomon man excavated from Futsukaichi cave (Futsukaichi city, Oita Prefecture, Japan), which is in the vicinity of Hegi cave, was not developed [36]. The period from 4,000 to 4,500 years ago, which was defined as the Late Jomon Period in the present study, was a time of decreasing temperatures in the Holocene world [21]. This was a time when it became difficult to obtain food, and many settlements in other parts of Japan were reported to have disappeared [20]. On the other hand, it was also a time when the sea level was higher than in the Initial/Early Jomon Period and coastline was within approximately 7 kilometers of Hegi cave, in which the Jomon human remains analyzed were found. Freshwater shellfish, such as river snails, have been found in the strata at which Initial/Early Jomon humans were found, while brackish water shellfish, including clams, were detected in the strata at which Late Jomon humans were discovered [18]. This suggests that by the Late Jomon period, the coastline was close enough for people to travel to food gathering from the Hegi caves. This may have contributed to the expansion of the range of activities during this period. The degree of development of the linea aspera may reflect these changes in the living environment. The weight of the archaic man may be estimated from the diameter of the femoral head and the height from the length of the femur. We measured the femoral head diameter and diaphyseal length of all bones used in the present study and examined their relationships. No correlations were found in modern humans, whereas correlations were noted in Initial/Early and Late Jomon humans ($r = 0.63$ and 0.99, respectively). The correlations observed in Late Jomon humans are of interest because they suggest that humans had a uniform body shape that was never obese due to the scarcity of food; however, the small sample size examined may be a factor. The mean values for many of the diaphyseal cross-sectional morphologies were grouped in the order of the modern, Initial/Early Jomon, and Late Jomon populations, and the distribution of points in the principal component analysis was also grouped in this order. In terms of the forward curvature, the mean values for the modern and Initial/Early Jomon populations were similar, while the mean

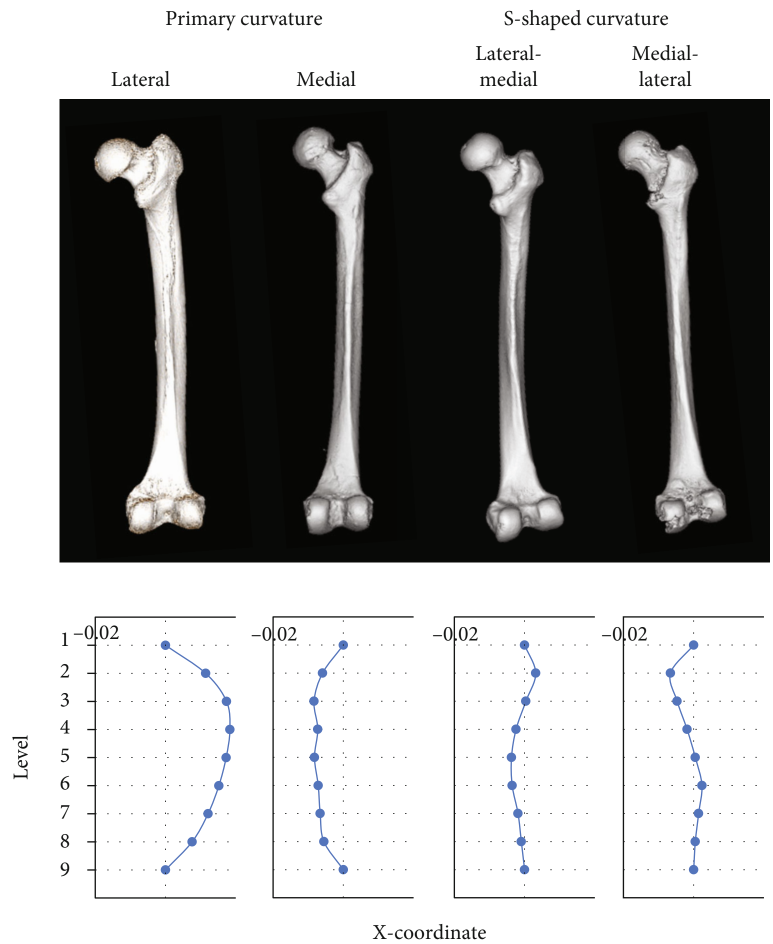

Figure 8: Examples of four types of the lateral curvature.

Table 3: Types of femoral curvatures. The proportions of each type of curvature significantly differed among modern, Initial/Early, and Late Jomon Period populations.

	Primary curvature		S-shaped curvature	
	Lateral	Medial	Lateral-medial	Medial-lateral
Modern	19	4	23	0
Initial/Early Jomon	0	3	0	7
Late Jomon	0	0	1	4

value for Late Jomon population was significantly higher. This suggests that these indices are factors that are influenced by the same living environment, and these data provide an important basis for future comparisons with other populations.

In terms of the lateral curvature, modern and Jomon femurs showed very different patterns. The pattern of curvature was consistent with the axis connecting the center points of the cross-sections at levels 1 and 9, with some showing the primary curvature with the center point of the other level consistently on the outside or inside, and some showing the S-shaped curvature with respect to the axis, with the outside at the top and the inside at the bottom or the inside at the top and the outside at the bottom. In modern humans, 23 out of the 46 femurs measured showed the primary curvature, while those that showed the S-shaped curvature all curved laterally at the top. In contrast, the Initial/Early and Late Jomon populations both showed a more S-shaped curvature and the pattern was mostly medial at the top. In terms of the average degree of curvature, modern humans showed the lateral curvature at the top and almost along the axis at the bottom. A columnar material generally undergoes strain when loaded along its axis. Euler's buckling theory is a qualitative and quantitative description of the form and magnitude of strain [37]. The hip joint has a degree of freedom of lateral rotation, while the knee joint has a fixed degree of freedom of lateral rotation. Applying this combination of degrees of freedom at the hip and knee joints to the theory predicts lateral curvature at the top region and alignment with the bone axis at the bottom region. The results of the present measurements were in good agreement with this prediction. In the case of the anterior curvature, both the hip and knee joints have a degree of freedom in the direction of forward rotation; therefore, the center of the diaphysis is the apex of the curvature, a result that is consistent with this theory. On the other hand, the

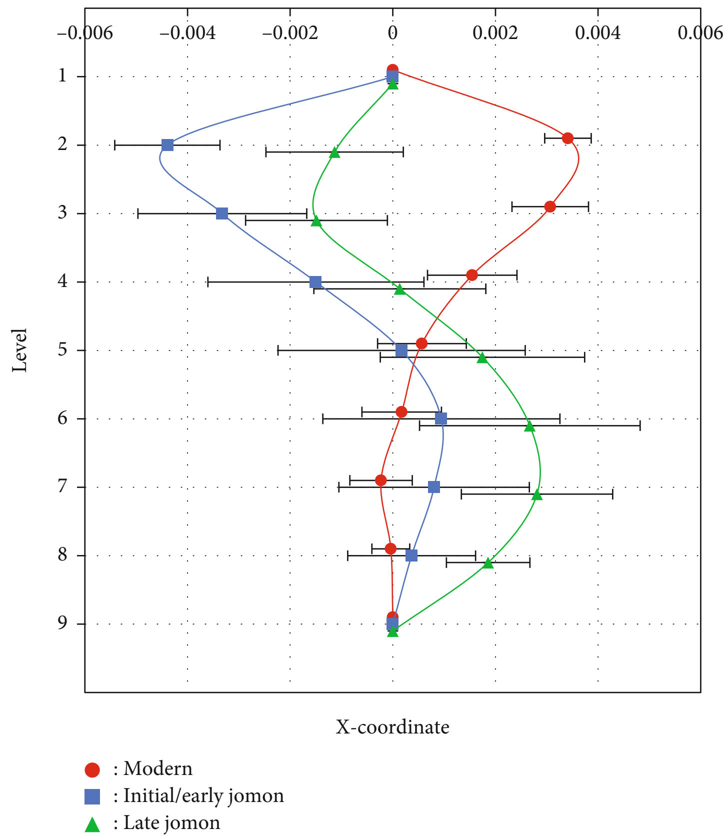

Figure 9: Averages of x-coordinates of modern, Initial/Early Jomon, and Late Jomon Period populations. Averages are plotted at each cross-sectional level. Error bars indicate ±1 standard error.

S-shaped curvature occurs when the hip or knee joint is fixed, and the other joint has a degree of freedom in the lateral direction. If the upper part of the body is flexed laterally, the hip joint may have a lateral degree of freedom or the knee joint may have a degree of freedom in the medial direction. If the upper part of the body is flexing medial at the top, it must have freedom in the opposite direction. The hip joint may tilt laterally when loaded, possibly due to Trendelenburg's sign of abductor weakness. Although the femurs excavated from Hegi cave showed no morphological feature to suggest this pathological condition, an imbalance between the abductor and adductor muscles may cause lateral thrust in the hip joint. In knee osteoarthritis, the knee moves laterally in the case of a medial deformity and medially in the case of a lateral deformity [38]. This lateral and medial thrust may explain the difference in S-shaped patterns between modern and Jomon femurs. Previous studies on European descendants reported that the incidence and types of knee joint diseases were influenced by the historical time [39, 40]. The frequency of patellofemoral osteoarthritis was found to be higher in Asian hunter-gatherers [41]. These findings indicate differences in lifestyle between the modern and Jomon populations that affected the curvature of the femur through differences in the incidence of knee joint diseases. The present results suggest that Jomon humans had more developed adductor muscles than modern humans; however, further investigations on the abductor muscles and the state of the knee joint using other markers are needed. Moreover, a biomechanical analysis using the finite element method is warranted to examine how this difference in the lateral curvature pattern contributed to the robustness of the Jomon Period femur or whether it was a pathological condition.

5. Conclusion

The method used in the present study to quantify the morphological characteristics of cortical bone in the femur diaphysis based on CT images revealed marked differences between modern and Jomon Period bones excavated from Hegi cave. The results obtained showed not only differences between the modern and Jomon populations but also among the Initial/Early and Late Jomon Periods according to age. Some of the indices measured exhibited different patterns between the modern and Jomon populations, while others were similar between the modern and Initial/Early Jomon Period populations, but different from the Late Jomon Period population. These differences strongly suggest the influence of different mechanisms on the morphological characteristics of each femur. Climate change and marine transgression during the Late Holocene are strong candidates for explaining the differences observed between the Initial/Early and Late Jomon Period populations. The further application of this method to different paleoanthropological populations is expected to yield novel insights.

Data Availability

Previously reported morphological data of modern Japanese people were used to support this study and are available at doi:10.1111/joa.13399 and doi:10.1111/joa.13060. These prior studies are cited at relevant places within the text as references [9, 10].

Conflicts of Interest

The authors declare that there is no conflict of interest regarding the publication of this manuscript.

Acknowledgments

We would like to thank the Department of Forensic Pathology and Science, Graduate School of Biomedical Sciences, Nagasaki University, for maintaining the clinical multislice CT used in this study. This work was supported by a Grant-in-Aid for Scientific Research (B) from the Ministry of Education, Culture, Sports, Science and Technology, Japan (grant number 22370087).

References

[1] J. E. Hagen, A. N. Miller, S. M. Ott et al., "Association of atypical femoral fractures with bisphosphonate use by patients with varus hip geometry," *Journal of Bone & Joint Surgery -American*, vol. 96, no. 22, pp. 1905–1909, 2014.

[2] Y. Oh, Y. Wakabayashi, Y. Kurosa, M. Ishizuki, and A. Okawa, "Stress fracture of the bowed femoral shaft is another cause of atypical femoral fracture in elderly Japanese: a case series," *Journal of Orthopaedic Science*, vol. 19, no. 4, pp. 579–586, 2014.

[3] J. Starr, Y. K. Tay, and E. Shane, "Current understanding of epidemiology, pathophysiology, and management of atypical femur fractures," *Current Osteoporosis Reports*, vol. 16, no. 4, pp. 519–529, 2018.

[4] I. T. Haider, P. S. Schneider, and W. B. Edwards, "The role of lower-limb geometry in the pathophysiology of atypical femoral fracture," *Current Osteoporosis Reports*, vol. 17, no. 5, pp. 281–290, 2019.

[5] K. Hyodo, T. Nishino, H. Kamada, D. Nozawa, H. Mishima, and M. Yamazaki, "Location of fractures and the characteristics of patients with atypical femoral fractures: analyses of 38 Japanese cases," *Journal of Bone and Mineral Metabolism*, vol. 35, no. 2, pp. 209–214, 2017.

[6] J. W. Kim, J. J. Kim, Y. S. Byun et al., "Factors affecting fracture location in atypical femoral fractures: a cross-sectional study with 147 patients," *Injury*, vol. 48, no. 7, pp. 1570–1574, 2017.

[7] G. Holzer, G. von Skrbensky, L. A. Holzer, and W. Pichl, "Hip fractures and the contribution of cortical versus trabecular bone to femoral neck strength," *Journal of Bone and Mineral Research*, vol. 24, no. 3, pp. 468–474, 2009.

[8] K. J. Jepsen, E. M. Bigelow, and S. H. Schlecht, "Women build long bones with less cortical mass relative to body size and bone size compared with men," *Clinical Orthopaedics and Related Research*, vol. 473, no. 8, pp. 2530–2539, 2015.

[9] T. Imamura, T. Tsurumoto, K. Saiki et al., "Morphological profile of atypical femoral fractures: age-related changes to the cross-sectional geometry of the diaphysis," *Journal of Anatomy*, vol. 235, no. 5, pp. 892–902, 2019.

[10] T. Imamura, K. Ogami-Takamura, K. Saiki et al., "Morphological divergence in the curvature of human femoral diaphyses: tracing the central mass distributions of cross-sections," *Journal of Anatomy*, vol. 239, no. 1, pp. 46–58, 2021.

[11] D. Endo, K. Ogami-Takamura, T. Imamura et al., "Reduced cortical bone thickness increases stress and strain in the female femoral diaphysis analyzed by a CT-based finite element method: implications for the anatomical background of fatigue fracture of the femur," *Bone Reports*, vol. 13, p. 100733, 2020.

[12] W. Bruns, M. Bruce, G. Prescott, and N. Maffulli, "Temporal trends in femoral curvature and length in medieval and modern Scotland," *American Journal of Physical Anthropology*, vol. 119, no. 3, pp. 224–230, 2002.

[13] A. Yamanaka, H. Gunji, and H. Ishida, "Curvature, length, and cross-sectional geometry of the femur and humerus in anthropoid primates," *American Journal of Physical Anthropology*, vol. 127, no. 1, pp. 46–57, 2005.

[14] S. Pfeiffer, M. E. Cameron, J. Sealy, and A. C. Beresheim, "Diet and adult age-at-death among mobile foragers: a synthesis of bioarcheological methods," *American Journal of Physical Anthropology*, vol. 170, no. 1, pp. 131–147, 2019.

[15] J. Wolff, *The Law of Bone Remodelling (trans: Maquet P, Furlong R)*, Springer, New York, 1986.

[16] M. E. Ballard, "Anterior femoral curvature revisited: race assessment from the femur," *Journal of Forensic Sciences*, vol. 44, no. 4, pp. 700–707, 1999.

[17] L. L. Shackelford and E. Trinkaus, "Late Pleistocene human femoral diaphyseal curvature," *American Journal of Physical Anthropology*, vol. 118, no. 4, pp. 359–370, 2002.

[18] Y. Naito, "Hegi-Doketsu no jinkotsu," in *Honyabakeityoushi*, pp. 85–96, Honyabakeityoushikankoukai, Oita, Japan, 1991.

[19] M. Yoneda, A. Saso, R. Suzuki et al., "Chronology of the Yayoi skeletal remains from the Kanto district, Japan: a preliminary re-evaluation by radiocarbon dating of postcranial material," *Anthropological Science*, vol. 113, no. 2, pp. 169–182, 2005.

[20] L. Fenggui, Z. Yili, F. Zhaodong, H. Guangliang, Z. Qiang, and Z. Haifeng, "The impacts of climate change on the Neolithic cultures of Gansu-Qinghai region during the late Holocene Megathermal," *Journal of Geographical Sciences*, vol. 20, no. 3, pp. 417–430, 2010.

[21] H. Kawahata, "Climatic reconstruction at the Sannai-Maruyama site between Bond events 4 and 3—implication for the collapse of the society at 4.2 ka event," *Progress in Earth and Planetary Science*, vol. 6, no. 1, p. 63, 2019.

[22] M. Minagawa, D. A. Winter, and I. R. Kaplan, "Comparison of Kjeldahl and combustion methods for measurement of nitrogen isotope ratios in organic matter," *Analytical Chemistry*, vol. 56, no. 11, pp. 1859–1861, 1984.

[23] H. Matsuzaki, C. Nakano, Y. Sunohara-Tsuchiya et al., "Multinuclide AMS performances at MALT," *Nuclear Instruments and Methods in Physics Research Section B: Beam Interactions with Materials and Atoms*, vol. 259, no. 1, pp. 36–40, 2007.

[24] S. L. Brock and C. B. Ruff, "Diachronic patterns of change in structural properties of the femur in the prehistoric American Southwest," *American Journal of Physical Anthropology*, vol. 75, no. 1, pp. 113–127, 1988.

[25] P. Pottecher, K. Engelke, L. Duchemin et al., "Prediction of hip failure load: in vitro study of 80 femurs using three imaging methods and finite element models-the European fracture

study (EFFECT)," *Radiology*, vol. 280, no. 3, pp. 837–847, 2016.

[26] S. H. Lee, Y. H. Lee, and J. S. Suh, "Lateral cortical thickening and bone heterogeneity of the subtrochanteric femur measured with quantitative CT as indicators for early detection of atypical femoral fractures in long-term bisphosphonate users," *American Journal of Roentgenology*, vol. 209, no. 4, pp. 867–873, 2017.

[27] H. Scherf and R. Tilgner, "A new high-resolution computed tomography (CT) segmentation method for trabecular bone architectural analysis," *American Journal of Physical Anthropology*, vol. 140, no. 1, pp. 39–51, 2009.

[28] Y. Deng, L. Wang, C. Zhao et al., "A deep learning-based approach to automatic proximal femur segmentation in quantitative CT images," *Medical and Biological Engineering and Computing*, vol. 60, pp. 1417–1429, 2022.

[29] T. D. Stewart, "Anterior femoral curvature: its utility for race identification," *Human Biology*, vol. 3, pp. 49–62, 1962.

[30] K. Kimura, "Anterior femoral curvature in the Japanese and the Ainu," *Journal of Anthropological Society of Nippon*, vol. 81, no. 2, pp. 103–112, 1973.

[31] J. Ikeda, "Jomonjidaijin no hensen," in *Nihonjin no kigen*, pp. 114–135, Kodansya, Tokyo, Japan, 1982.

[32] T. Ogata, *Jomonjidaijinkotsu*, Jinruigaku Koza, Yuzankaku, Tokyo, Japan, 1981.

[33] B. Yanaguchi, "A review of the osteological characteristics of the Jomon population in prehistoric Japan," *Journal of Anthropological Society of Nippon*, vol. 90, pp. 77–90, 1982.

[34] K. Okazaki, "Habitual behaviors in the Jomon people, based on the analysis of the external cross sections of juvenile limb bones," *Anthropological Science (Japanese Series)*, vol. 115, no. 2, pp. 109–125, 2007.

[35] E. Trinkaus, C. B. Ruff, S. E. Churchill, and B. Vandermeersch, "Locomotion and body proportions of the Saint-Césaire 1 Châtelperronian Neandertal," *Proceedings of the National Academy of Sciences of the United States of America*, vol. 95, no. 10, pp. 5836–5840, 1998.

[36] T. Wakebe, K. Saiki, K. Okamoto, and S. Nagashima, "Ooita-ken Kokonoetyo Futsukaichishi syutudo no Jomonjidaizinkotsu," in *Kokonoetyo bunkazaityousahoukoku vol.27*, Kokonoetyou, Oita, Japan, 2004.

[37] B. G. Johnston, "Column buckling theory: historic highlights," *Journal of Structural Engineering*, vol. 109, no. 9, pp. 2086–2096, 1983.

[38] Y. Kuroyanagi, T. Nagura, Y. Kiriyama et al., "A quantitative assessment of varus thrust in patients with medial knee osteoarthritis," *The Knee*, vol. 19, no. 2, pp. 130–134, 2012.

[39] T. Waldron, "Changes in the distribution of osteoarthritis over historical time," *International Journal of Osteoarcheology*, vol. 5, no. 4, pp. 385–389, 1995.

[40] I. J. Wallace, S. Worthington, D. T. Felson et al., "Knee osteoarthritis has doubled in prevalence since the mid-20th century," *Proceedings of the National Academy of Sciences of the United States of America*, vol. 114, no. 35, pp. 9332–9336, 2017.

[41] K. Inoue, S. Hukuda, P. Fardellon et al., "Prevalence of large-joint osteoarthritis in Asian and Caucasian skeletal populations," *Rheumatology*, vol. 40, no. 1, pp. 70–73, 2001.

Hindawi
BioMed Research International
Volume 2022, Article ID 5765604, 9 pages
https://doi.org/10.1155/2022/5765604

Research Article

Dental Calculi of Siberian Natives, Russian Settlers, and Korean People of Joseon Dynasty Period in the 16th to 19th Century Eurasia Continent

Hyejin Lee,[1,2] **Jong Ha Hong**,[3] **Larisa Tataurova**,[4] **Sergey Slepchenko**,[5] **Jieun Kim**,[6] **and Dong Hoon Shin**[6]

[1]*Department of Forensic Medicine, Seoul National University College of Medicine, Seoul, Republic of Korea*
[2]*Ministry of National Defense Agency of KIA Recovery & Identification, Seoul, Republic of Korea*
[3]*Institute of Korean Archaeology and Ancient History, Kyung Hee University, Seoul, Republic of Korea*
[4]*Federal State Budgetary Institution of Science Institute of Archaeology and Ethnography of the Siberian Branch of the Russian Academy of Sciences, Omsk, Russia*
[5]*Tyumen Scientific Center of the Siberian Branch of the Russian Academy of Sciences, Tyumen, Russia*
[6]*Department of Anatomy and Cell Biology, Seoul National University College of Medicine, Seoul, Republic of Korea*

Correspondence should be addressed to Sergey Slepchenko; s_slepchenko@list.ru and Dong Hoon Shin; cuteminjae@gmail.com

Received 21 November 2021; Accepted 19 April 2022; Published 9 May 2022

Academic Editor: Andrey Cherstvy

Objective. The prevalence of calculus is known to be variable by difference in diets or subsistence strategy between human populations. However, this situation has not been confirmed so far for hunter-gatherers and farming people in terms of history. In this study, we tried to reveal the association of diets or subsistence with calculus in different historical populations: Siberian natives, Joseon period Korean people, and Russian settlers in Siberia. *Design.* We examined the teeth of Siberian natives (hunter-gatherers), Russian (wheat farming) settlers, and Joseon (rice farming) people in sixteenth to nineteenth century. Age and sex were estimated using the methods of Buikstra and Ubelaker (1994). We examined specimens to detect signs of calculus formation in teeth. Calculus rates in each group were statistically compared, and the proportions of calculus by age or sex were also compared across each group. We used package R for statistical analysis. *Results and Discussion.* The prevalence of calculus deposition decreased in the order of Joseon people, Russian settlers, and Siberian natives. Our study proposes that the rate of calculi among farming people was evidently higher than that of hunter-gatherers in sixteenth to nineteenth century Eurasia. In all three groups, calculus prevalence became higher as age increases and was noteworthy in males. *Conclusion.* Current study demonstrated a significant difference of calculus formation between those groups with different diets or subsistence strategies. Higher prevalence of dental calculus was observed in agriculturalist Joseon Koreans and Russian settlers, but Siberian natives exhibited relatively lower frequency of dental calculus. The results of this study enable us to reconsider the meaning of association between subsistence strategy and calculus in different historical populations.

1. Introduction

Calculus is mineralized material on tooth surface that is covered by bacterial plaque. In general, it is the primary agent for various dental pathologies such as caries, periodontitis, and alveolar abscess [1–4]. The conditions that can affect calculus are very diverse [2, 5, 6]. Many factors like salivary flow, hydration, mineral and silicon content in food and water, and oral hygiene are known to affect the prevalence and extent of dental calculus in individuals. Clinical and experimental data also supported that urea and alkaline pH might induce calculus mineralization as well [7–9].

Besides them, the dietary pattern of specific population is one of the most serious causes of dental calculus forming [10]. Briefly, calculus forming might have been related to protein-rich food like fish or meat [7, 11, 12]. Others argued that carbohydrate-rich diets might promote calculus deposition [7, 13, 14]. Calculus is also facilitated by severe dental attrition that is known to be highly influenced by the type of food we eat [15–20]. Therefore, the association between specific populations' subsistence strategy and tooth pathology has been studied in different populations [21–28]. For example, the causal relationship between carbohydrates and caries has been discussed extensively. The more carbohydrate-rich foods they eat, the more cavities they might have [24, 29–36]. Likewise, the prevalence of calculus could be variable according to the difference in subsistence strategy and lifestyle of specific population [7]. However, the data of this situation, which could reveal information regarding the dental health and hygiene level of specific historical populations, has not been well established so far in terms of history.

The sixteenth to nineteenth century Eurasian continent is therefore an interesting topic for us. Since the wave of modernization was not yet dominated on the eastern part of continent until then, there were various population groups in this world that maintained their survival in very traditional ways. That is, the Siberian native people lived with hunting and gathering technique that had been handed down for generations. Many other people were also engaged in agriculture in Eurasian continent during the same period. Rice farming was a major production base for those Korean or Japanese people in East Asia. Russian settlers, mainly depending on wheat farming and lived relatively rudimentary, but under the clear influence of Russian Empire, also existed in Siberia. Although they existed in similar time and on the same Eurasian continent, they maintained completely different dietary and survival strategy. Since this means that the occurrence of calculus might have been quite different between them, we tried to reveal it with any scientific evidence.

2. Materials and Methods

We examined the crania of West Siberian natives, Russian settlers, and Joseon period Korean people (Figure 1). All three groups were living in the sixteenth to nineteenth century. The archaeological information of Siberian natives, Russian settlers, and Joseon period mummies are summarized in Table 1 and Figure 1. As for the West Siberian natives, the crania have been curated by the Institute of the Problems of Northern Development Center (Tyumen, Russian Federation) [37]. The Siberian natives were hunter-gatherers. Their crania ($n = 53$; 30 females and 23 males) were originated from the Tatar ($n = 34$), Khanty ($n = 7$), and Nenet ($n = 12$) people (Table 1 and Figure 1). The total number of Siberian natives' teeth was 820. Among them, the Tatars, a Turkic-speaking people of West Siberia, were fishermen, hunters, and pastoralists [38]. The Khanty (fishermen and hunters) settled in north-taiga or forest-tundra zones at the Middle and Lower Ob River regions [39, 40]. The Nenets, as hunters, fishermen, and reindeer herders, lived at the Arctic and Near Arctic Circle [37, 41].

Meanwhile, the Russian settler's crania investigated in this study were consisted of 79 individuals (32 males and 47 females; total number of teeth = 1,304) (Table 1 and Figure 1). The Russian settlers' Izyuk village was built as early as 1648 CE around the Irtysh River [37]. A cemetery was found during archaeological excavation for the site. In previous reports, the settlers buried at the cemetery migrated from Central or Northern Russia as well as Eastern Europe [37, 42]. They were engaged in wheat cultivation. Their crania were curated in the Institute of the Problems of Northern Development Center (Tyumen, Russia) [37].

The Joseon dynasty people's crania were consisted of 90 individuals (48 males and 42 females; total number of teeth = 1,992) (Table 1 and Figure 1). They were engaged in rice cultivation. Joseon dynasty was one of the last countries to open its ports to Western countries. Therefore, our study on Joseon people's teeth can be a good example of dental pathology in a country where sociocultural changes by industrialization were delayed until relatively recent days [30]. The crania are curated in Seoul National University College of Medicine (Seoul, South Korea).

Age and sex were estimated by methods of Buikstra and Ubelaker [43]. Age estimation was based on pubic symphysis, auricular surface, ectocranial suture closure, and level of dental attrition. The age of immature remains was estimated using dental eruption and formation and epiphyseal closure of long bones. All individuals were grouped into 4 age categories for more detailed analysis: adolescents (15-19 years), young adults (20-34 years), middle adults (35-49 years), and old adults (over 50).

Sex was also estimated using dimorphic features in pelvis or skull, as these are reliable data for sex determination in osteoarchaeology. Skull's sexually dimorphic features include mastoid process, nuchal crest, inion protuberance, zygomatic root, supraorbital ridge, frontal shape, and gonial shape [44–47]. Dimorphic features of the pelvis also include ventral arc, preaurciular sulcus, greater sciatic notch, medial portion of the pubis, subpubic concavity, subpubic angle, and median ischiopubic ridge [47, 48]. The information of age and sex distributions for Siberian natives, Russian settlers, and Joseon people are summarized in Supplementary Tables 1 and 2, respectively.

Before our examination, every tooth was cleaned with soft brush to facilitate precise observation. All individuals were examined for any signs of calculus formation. Dental calculi were evaluated macroscopically under natural light with the aid of magnifying glass. Calculus was documented by the standards of Brothwell [45] and Buikstra and Ubelaker [43]. Two methods of analysis of dental calculi were used in this study, individual count method (per individual) and tooth count method (per teeth) [49]. Per individual method is useful in studying the population prevalence of a certain dental disease, and per teeth method permits larger sample sizes for statistical analysis and facilitates the comparison of disease frequencies [49]. The prevalence of calculi was also analyzed by sex and age to see any difference between them.

In this study, package R [50] was used for statistical analysis. We compared the proportions of age or sex across each group by Pearson's Chi-squared test [37]. The calculus rates in each group were compared by Pearson Chi-squared test.

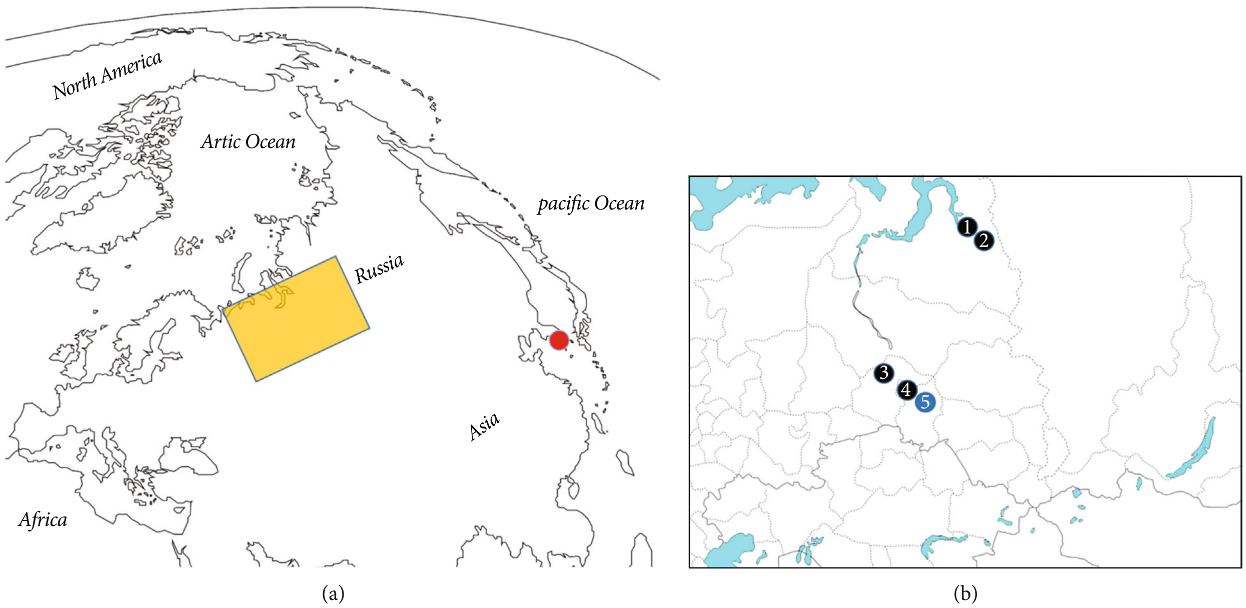

Figure 1: The geographic location of archaeological sites for each group studied in this research. (a) The red circle indicates South Korea. Yellow rectangle indicates the excavation sites of native and Russian settlers. (b) Magnified image of yellow rectangle part in (a). Black dots represent the sites of Siberian natives (1 and 2, Nenet; 3, Khanty; 4, Tatar). The blue dot indicates the excavation site (Izyuk, Omsk) for Russian settlers.

Table 1: Archaeological information.

People	Site	Date	N	Activity and subsistence
Siberian natives				
Tatar	Omsk	17th to 20th century	34	Fishers-hunters, cattle breeder, farmers to a lesser extent
Khanty	Khanty-Mansi autonomous Okrug	17th to 18th century	7	Fishers-hunters
Nenet	Yamalo-Nenets autonomous Okrug	19th to 20th century	12	Fishers, reindeer herders
Russian settlers				
Russian	Omsk (Izyuk)	16th to 18th century	79	Agricultural (wheat)
Joseon period people				
Korean	South Korea	16th to 19th century	90	Agricultural (rice)

For comparison of prevalence in case that sample number was less than 10, Fisher's exact test was applied [37]. We used the package ggplot2 implemented in package R version 4.0.2 (R Foundation for Statistical Computing, Vienna, Austria) to draw charts for displaying prevalence of data in each group [51].

3. Results and Discussion

In statistical analysis to see the homogeneity in the age proportions, we confirmed that the age groups between Siberian natives, Russian settlers, and Joseon period Koreans were not differently distributed (Pearson's Chi-squared test, P value = 0.3225 and 0.217 for Siberian natives and Russian settlers and Russian settlers and Joseon people, respectively; Fisher's exact test, P value = 0.1507 for Siberian natives and Joseon people). Likewise, sex proportions showed no intergroup difference statistically between them (Pearson's Chi-squared test, P value = 0.1013, 0.3297, and 0.5157 for between Siberian natives and Russian settlers, Siberian natives and Joseon people, and Russian settlers and Joseon people, respectively).

In this study, the prevalence of calculus deposition *by individual* decreased in the order of Joseon people (76.7%), Russian settlers (60.8%), and Siberian natives (26.4%) (Table 2). Also, in the prevalence of calculus *by teeth*, the

Table 2: Calculus prevalence of Siberian natives, Russian settlers, and Joseon period people (per individual).

Age	Siberian natives				Russian settlers				Joseon people			
	Total (n)	Affected (n)	Nonaffected (n)	Frequency (%)	Total (n)	Affected (n)	Nonaffected (n)	Frequency (%)	Total	Affected (n)	Nonaffected (n)	Frequency (%)
Adolescent	7	1	6	14.3	9	4	5	44.4	4	3	1	75.0
YA	26	6	20	23.1	30	23	7	76.7	38	27	11	71.1
MA	16	6	10	37.5	26	16	10	61.5	37	31	6	83.8
OA	4	1	3	25.0	14	5	9	35.7	11	8	3	72.7
Total	53	14	39	26.4	79	48	31	60.8	90	69	21	76.7

Table 3: Calculus prevalence of Siberian natives, Russian settlers, and Joseon period people (*per teeth*).

Age	Siberian natives				Russian settlers				Joseon people			
	Total (n)	Affected (n)	Nonaffected (n)	Frequency (%)	Total (n)	Affected (n)	Nonaffected (n)	Frequency (%)	Total	Affected (n)	Nonaffected (n)	Frequency (%)
Adolescent	121	2	119	1.7	138	16	122	11.6	116	21	95	18.1
YA	391	10	381	2.6	611	158	453	25.9	942	244	698	25.9
MA	242	38	204	15.7	400	106	294	26.5	783	314	469	40.1
OA	66	4	62	6.1	155	15	140	9.7	151	69	82	45.7
Total	820	54	766	6.6	1,304	295	1,009	29.2	1,992	648	1,344	32.5

Table 4: Statistical analysis of dental calculus prevalence between Siberian natives, Russian settlers, and Joseon people (Chi-squared test; *P* value).

	Siberian natives	Russian settlers	Joseon people
Siberian natives		[a] < 2.2e-16∗∗∗∗	[a] < 2.2e-16∗∗∗∗
Russian settlers	[a] 0.0002175∗∗∗		[a] 9.669e-10∗∗∗∗
Joseon people	[a] 1.159e-08∗∗∗∗	[a] 0.03859∗	

Per individual for lower left cells; *per teeth* for upper right cells. [a]Chi-squared test.

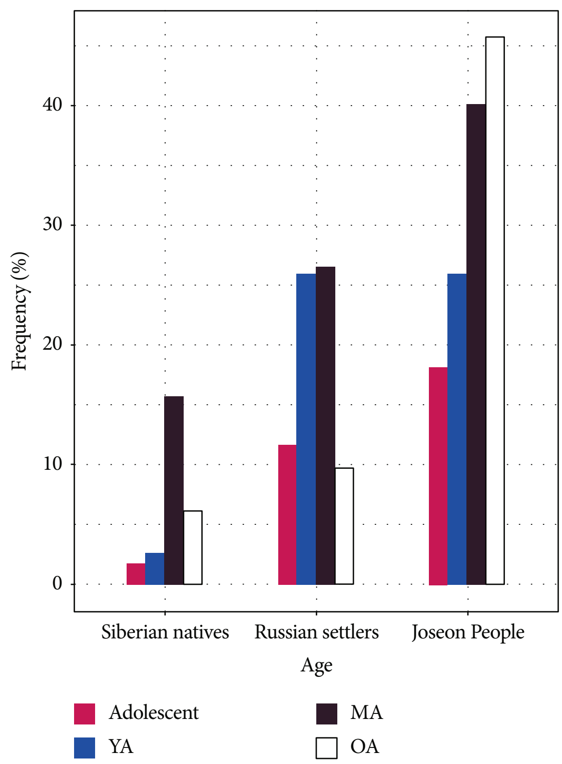

Figure 2: The analysis of calculus rates by age. Red, blue, black, and white bars indicate adolescents, young adults, middle adults, and old adults in each group, respectively. The calculus prevalence per teeth generally increases as age increases in Siberian natives, Russian setters, and Joseon people groups. This phenomenon is particularly remarkable in the process of aging from adolescence to middle adult, but is decreasing in old adult.

order was the same as seen in the prevalence by individual: Joseon people (32.5%), Russian settlers (29.2%), and Siberian natives (6.6%) (Table 3). In particular, the Siberian natives differed greatly from the other two groups in calculus prevalence. The differences between each group *by individual* were statistically significant (Chi-squared: for Joseon people and Russian settlers, $P = 0.03859$; for Joseon people and Siberian natives, $P = 1.159e-08$; for Russian settlers and Siberian natives, $P = 0.0002175$) (Table 4). The differences between three groups *by teeth* were also statistically significant (Chi-squared: for Joseon people and Russian settlers, $P = 9.669e-10$; for Joseon people and Siberian natives, $P < 2.2e-16$; for Russian settlers and Siberian natives, $P < 2.2e-16$). The Chi-squared test results for calculus prevalence by individual and teeth are summarized in Table 4.

While there are many factors involved in the generation of calculus, diets have long been a part of major interest in related research [11, 13].

Joseon people and Russian settlers in this study must have had a nutrition based primarily on agricultural crops (mainly rice or wheat) with some meat, while Siberian natives mostly relied on animal products for their nutrition. The result of our study to compare agricultural (Joseon and Russian) and hunter-gatherer (native Siberians) populations suggests that an increase in carbohydrate intake might have had an important role in calculus formation in sixteenth to eighteenth century Eurasian continent.

As for the analysis of calculus rates by age, as seen in Figure 2, the calculus prevalence *per teeth* generally increases as age increases in all Siberian native, Russian setters, and Joseon period groups. This phenomenon is particularly noticeable in the process of aging from adolescence to middle adult. However, we also note that the prevalence of calculus *per teeth*, which continued to increase until the middle adult, has been observed to decrease in old adult (Figure 2). We conjecture that this might have been caused by the effect of antemortem tooth loss in old age on dental calculus. This increasing pattern as age increases was not remarkable in the calculus prevalence *per individual*.

As for the analysis of calculus rates by sex, the prevalence of calculus deposition in males was noteworthy in all three groups (Table 5). In Siberian natives, calculus was found in 47 out of 422 male teeth (11.1%) while 7 out of 398 female teeth (1.8%). The calculus prevalence was statistically different between both sexes (Chi-squared test, $P = 1.358e-07$). In case of Russian settler's teeth, we found 141 calculi out of 565 male teeth (25.0%) and 154 calculi out of 739 female teeth (20.8%). The difference was not statistically significant (Chi-squared test, $P = 0.09028$) (Table 5). In case of Joseon people, calculus was observed in 392 out of 1,112 male teeth (35.3%), while 256 out of 880 female teeth (29.1%). The difference in calculus frequency between sex was statistically confirmed (Chi-squared test, $P = 0.00415$) (Table 5). Higher prevalence of calculus in males than females appeared that the former had a dietary or behavioral practice that contributed to calculi formation or perhaps poorer oral hygiene than their female counterparts.

As mentioned above, in anthropological studies on past populations, it has been proposed that diets or subsistence strategy had impact on the prevalence of dental calculus [7, 10–20]. Such calculus-related studies have been also performed on modern people [2]. For instance, Gaare et al.'s report [52] on twentieth century student groups from Norway and Indonesia, for which variables like age, sex, and

Table 5: Prevalence of calculus per teeth by sex (Chi-squared test).

	Male			Female			P value
	Affected (n)	Non-affected (n)	Frequency (%)	Affected (n)	Nonaffected (n)	Frequency (%)	
Siberian natives	47	375	11.1	7	391	1.8	[a]1.358e-07****
Russian settlers	141	424	25.0	154	585	20.8	[a] 0.09028
Joseon people	392	720	35.3	256	624	29.1	[a] 0.00415**

[a]Chi-squared test.

tooth brushing could be easily controlled, is significant to understand the impacts of diets or subsistence strategy on dental calculus rates. According to the study, Indonesian students showed significantly higher calculus rate than that of the Norwegian students, which might be caused by their characteristics in diets, drinking waters, or eating habits [52]. The authors also speculated that diets can be the most significant causing factor in the formation of dental calculus considering that the Norwegian individual with Asian cultural background (e.g., dietary habit) represented higher calculus rate than the other Norwegians [52]. These preceding studies on archaeological and modern populations are certainly helpful in interpreting results from the current report.

4. Conclusion

This study on the prevalence of dental calculus is conducted on three different populations in the sixteenth to nineteenth century Eurasian continent: Siberian natives, Russian settlers, and Joseon period Korean people. All these groups maintained different diet strategies as wheat- and rice-farming agriculturalists and hunter-gatherers. In brief, Joseon period Koreans were living in rice-cultivating society of East Asia. Russian settlers were based primarily on wheat as a major crop with meats. Siberian natives mostly relied on animal products as hunter-gatherers. The current study demonstrated a significant difference of calculus formation between those three groups with different diets or subsistence strategy in Eurasian continent. Higher prevalence of dental calculus was observed in agriculturalist Joseon Koreans and Russian settlers, but Siberian natives exhibited relatively lower frequency of dental calculus. The results of this study enable us to consider the meaning of association between diets, subsistence strategy, and dental calculus in different populations in history once again.

Data Availability

The datasets used in the current study are available from corresponding author on reasonable request.

Conflicts of Interest

The authors declare that they have no conflicts of interest.

Acknowledgments

This work was supported by the Ministry of Education of the Republic of Korea and the National Research Foundation of Korea (NRF-2019S1A5C2A01083578); by the Education and Research Encouragement Fund of Seoul National University Hospital (2022), Korea; and by the State Task (program XII.186.4, project No. AAAA-A17-117050400143-4 of Tyumen Scientific Center SB RAS).

Supplementary Materials

Supplementary 1. Supplementary Table 1. Proportion of age in Siberian natives, Russian settlers, and Joseon people.

Supplementary 2. Supplementary Table 2. Proportion of sex in Siberian natives, Russian settlers, and Joseon people.

References

[1] S. W. Hillson, *Dental Anthropology*, Cambridge University Press, Cambridge, 2012.

[2] A. R. Lieverse, D. W. Link, V. I. Bazaliiskiy, O. I. Goriunova, and A. W. Weber, "Dental health indicators of hunter-gatherer adaptation and cultural change in Siberia's cis-Baikal," *American Journal of Physical Anthropology*, vol. 134, no. 3, pp. 323–339, 2007.

[3] J. R. Lukacs, "Dental paleopathology: methods for reconstructing dietary patterns," in *Reconstruction of life from the skeleton*, pp. 261–286, Wiley-Liss, New York, 1989.

[4] I. D. Mandel, "Calculus formation and prevention: an overview," *Compendium*, vol. 8, pp. S235–S241, 1987.

[5] C. S. Larsen, *Bioarchaeology: Interpreting Behavior from the Human Skeleton*, Cambridge University Press, United Kingdom, 2012.

[6] D. Ortner, *Identification of Pathological Conditions in Human Skeletal Remains*, Academic Press, Orlando, 2003.

[7] T. Delgado-Darias, J. Velasco-Vázquez, M. Arnay-de-la-Rosa, E. Martín-Rodríguez, and E. González-Reimers, "Calculus, periodontal disease and tooth decay among the prehispanic population from Gran Canaria," *Journal of Archaeological Science*, vol. 33, no. 5, pp. 663–670, 2006.

[8] S. R. Epstein, I. D. Mandel, and I. W. Scopp, "Salivary composition and calculus formation in patients undergoing hemodialysis," *Journal of Periodontology*, vol. 51, no. 6, pp. 336–338, 1980.

[9] L. Wong, "Plaque mineralization in vitro," *The New Zealand Dental Journal*, vol. 94, no. 415, pp. 15–18, 1998.

[10] R. Forshaw, "Dental indicators of ancient dietary patterns: dental analysis in archaeology," *British Dental Journal*, vol. 216, no. 9, pp. 529–535, 2014.

[11] A. R. Lieverse, "Diet and the aetiology of dental calculus," *International Journal of Osteoarchaeology*, vol. 9, no. 4, pp. 219–232, 1999.

[12] M. C. Lillie, "Mesolithic and Neolithic populations of Ukraine: indications of diet from dental pathology," *Current Anthropology*, vol. 37, no. 1, pp. 135–142, 1996.

[13] G. Flensborg, "Health and disease of hunter-gatherer groups from the eastern Pampa-Patagonia transition (Argentina) during the late Holocene," *Anthropological Science*, vol. 124, no. 1, pp. 29–44, 2016.

[14] J. Littleton and B. Frohlich, "An analysis of dental pathology and diet on historic Bahrain," *Paleorient*, vol. 15, no. 2, pp. 59–75, 1989.

[15] J. J. M. Damen and J. M. ten Cate, "Calcium phosphate precipitation is promoted by silicon," in *Recent advances in the study of dental calculus*, pp. 105–114, IRL Press, Oxford, 1989.

[16] C. Dawes, "Effects of diet on salivary secretion and composition," *Journal of Dental Research*, vol. 49, no. 6, pp. 1263–1272, 1970.

[17] G. Flensborg, "Paleopatologías bucales y tendencias paleodietarias en grupos cazadores-recolectores de la transición pampeano-patagónica oriental, durante el Holoceno tardío," *Relaciones de la Sociedad Argentina de Antropología*, vol. 38, no. 1, pp. 199–222, 2013.

[18] I. D. Mandel, "Biochemical aspects of calculus formation. I. Comparative studies of plaque in heavy and light calculus formers," *Journal of Periodontal Research*, vol. 9, no. 1, pp. 10–17, 1974.

[19] I. D. Mandel, "Biochemical aspects of calculus formation. II. Comparative studies of saliva in heavy and light calculus formers," *Journal of Periodontal Research*, vol. 9, no. 4, pp. 211–221, 1974.

[20] G. Rølla, D. Gaare, F. J. Langmyhr, and K. Helgeland, "Silicon in calculus and its potential role in calculus formation," in *Recent advances in the study of dental calculus*, pp. 97–103, IRL Press, Oxford, 1989.

[21] D. Fine and G. T. Craig, "Buccal surface wear of human premolar and molar teeth: a potential indicator of dietary and social differentiation," *Journal of Human Evolution*, vol. 10, no. 4, pp. 335–344, 1981.

[22] R. J. Hinton, "Form and patterning of anterior tooth wear among aboriginal human groups," *American Journal of Physical Anthropology*, vol. 54, no. 4, pp. 555–564, 1981.

[23] R. J. Hinton, "Differences in interproximal and occlusal tooth wear among prehistoric Tennessee Indians: implications for masticatory function," *American Journal of Physical Anthropology*, vol. 57, no. 1, pp. 103–115, 1982.

[24] C. S. Larsen, "Biological changes in human populations with agriculture," *Annual Review of Anthropology*, vol. 24, no. 1, pp. 185–213, 1995.

[25] P. F. Puech, "The diet of early man: evidence from abrasion of teeth and tools," *Current Anthropology*, vol. 20, no. 3, pp. 590–592, 1979.

[26] M. O. Smith, *Patterns of association between oral health status and subsistence: a study of aboriginal skeletal populations from the Tennessee Valley Area, [Ph.D. thesis]*, University of Tennessee, Knoxville, 1982.

[27] P. L. Walker, "A quantitative analysis of dental attrition rates in the Santa Barbara channel area," *American Journal of Physical Anthropology*, vol. 48, no. 1, pp. 101–106, 1978.

[28] P. L. Walker and J. M. Erlandson, "Dental evidence for prehistoric dietary change on the northern Channel Islands, California," *American Antiquity*, vol. 51, no. 2, pp. 375–383, 1986.

[29] A. H. Goodman, G. J. Armelagos, and J. C. Rose, "The chronological distribution of enamel hypoplasias from prehistoric Dickson mounds populations," *American Journal of Physical Anthropology*, vol. 65, no. 3, pp. 259–266, 1984.

[30] S. S. Han, K. W. Baek, M. H. Shin et al., "Dental caries prevalence of medieval Korean people," *Archives of Oral Biology*, vol. 55, no. 7, pp. 535–540, 2010.

[31] I. Herskovitz, "The evolution of oral microbiota and the spread of dental diseases," in *Digging for pathogens*, pp. 363–383, Balaban Publishers, Rehovot, 1998.

[32] S. W. Hillson, "Diet and dental disease," *World Archaeology*, vol. 11, no. 2, pp. 147–162, 1979.

[33] S. R. Saunders, C. De Vito, and M. A. Katzenberg, "Dental caries in nineteenth century upper Canada," *American Journal of Physical Anthropology*, vol. 104, no. 1, pp. 71–87, 1997.

[34] L. M. Sreebny, "Cereal availability and dental caries," *Community Dentistry and Oral Epidemiology*, vol. 11, no. 3, pp. 148–155, 1983.

[35] D. H. Temple and C. S. Larsen, "Dental caries prevalence as evidence for agriculture and subsistence variation during the Yayoi period in prehistoric Japan: biocultural interpretations of an economy in transition," *American Journal of Physical Anthropology*, vol. 134, no. 4, pp. 501–512, 2007.

[36] C. G. Turner II, "Dental anthropological indications of agriculture among the Jomon people of central Japan. X. Peopling of the Pacific," *American Journal of Physical Anthropology*, vol. 51, no. 4, pp. 619–635, 1979.

[37] H. J. Lee, J. H. Hong, Y. W. Hong, D. H. Shin, and S. M. Slepchenko, "Caries, antemortem tooth loss and tooth wear observed in indigenous peoples and Russian settlers of 16th to 19th century West Siberia," *Archives of Oral Biology*, vol. 98, pp. 176–181, 2019.

[38] S. M. Slepchenko, "Prevalence of caries among Siberian Tatars of the Omsk region in the 17th to early 20th centuries," *Archaeology Ethnology and Anthropology of Eurasia*, vol. 45, no. 3, pp. 146–154, 2017.

[39] A. N. Bagashyov, *Antropologiya Zapadnoj Sibiri*, Nauka408, Novosibirsk, 2017.

[40] E. V. Perevalova, *Severnye khanty: Etnicheskaia istoriia*, UrO RAN, Ekaterinburg, 2004.

[41] S. M. Slepchenko, A. A. Tsybankov, and V. Slavinsky, "Traditional living habits of the Taz tundra population: a paleoparasitological study," *The Korean Journal of Parasitology*, vol. 54, no. 5, pp. 617–623, 2016.

[42] L. Tataurova, *The mid rpe-Irtysh burial of the Russians in the 17th-19th centuries on the complex materials*, Ezuck-1, Omsk, 2010.

[43] J. E. Buikstra and D. H. Ubelaker, *Standards for data collection from human skeletal remains: proceedings of a seminar at the field museum of natural history*, Arkansas Archeological Survey, Fayetteville, 12154th edition, 1994.

[44] W. Bass, *Human Osteology: A Laboratory and Field Manual*, Missouri Archaeological Society, Columbia, 4th edition, 1995.

[45] D. R. Brothwell, *Digging Up Bones: The Excavation, Treatment and Study of Human Skeletal Remains*, Cornell University Press, Ithaca, NY, 3rd edition, 1981.

[46] D. Ferembach, I. Schwindezky, and M. Stoukal, "Recommendations for age and sex diagnoses of skeletons," *Journal of Human Evolution*, vol. 9, no. 7, pp. 517–549, 1980.

[47] B. S. Walter, S. N. DeWitte, and R. C. Redfern, "Sex differentials in caries frequencies in medieval London," *Archives of Oral Biology*, vol. 63, pp. 32–39, 2016.

[48] T. W. Phenice, "A newly developed visual method of sexing the os pubis," *American Journal of Physical Anthropology*, vol. 30, no. 2, pp. 297–301, 1969.

[49] S. Beckett and N. C. Lovell, "Dental disease evidence for agricultural intensification in the Nubian C-group," *International Journal of Osteoarchaeology*, vol. 4, no. 3, pp. 223–239, 1994.

[50] R Core Team, "*R: A language and Environment for Statistical Computing*," R Foundation for Statistical Computing, Vienna, Austria, 2017, https://www.R-project.org/.

[51] H. Wickham, *ggplot2: Elegant Graphics for Data Analysis*, Springer-Verlag, New York, 2009.

[52] D. Gaare, G. Rølla, and F. van der Ouderaa, "Comparison of the rate of formation of supragingival calculus in an Asian and European population," in *Recent advances in the study of dental calculus*, pp. 97–103, IRL Press, Oxford, 1989.

Hindawi
BioMed Research International
Volume 2021, Article ID 4884760, 11 pages
https://doi.org/10.1155/2021/4884760

Research Article

Significant Asymmetry of the Bilateral Upper Extremities of a Skeleton Excavated from the Mashiki-Azamabaru Site, Okinawa Island, Japan

Keiko Ogami-Takamura ,[1,2,3] Kazunobu Saiki,[1] Keita Nishi,[4] Tetsuaki Wakebe,[1,5] Daisuke Endo,[1] Kiyohito Murai,[1] Yoshiatsu Naito,[6†] and Toshiyuki Tsurumoto [1,2]

[1]*Department of Macroscopic Anatomy, Graduate School of Biomedical Sciences, Nagasaki University, 1-12-4 Sakamoto, Nagasaki, Nagasaki 852-8523, Japan*
[2]*Center of Cadaver Surgical Training, School of Medicine, Nagasaki University, 1-12-4 Sakamoto, Nagasaki, Nagasaki 852-8523, Japan*
[3]*Department of Anesthesiology and Intensive Care Medicine, Graduate School of Biomedical Sciences, Nagasaki University, 1-7-1 Sakamoto, Nagasaki, Nagasaki 852-8501, Japan*
[4]*Department of Oral Anatomy and Dental Anthropology, Graduate School of Biomedical Sciences, Nagasaki University, 1-7-1 Sakamoto, Nagasaki, Nagasaki 852-8588, Japan*
[5]*Nagasaki Medical College, 36-59 Atago, Nagasaki, Nagasaki 850-0822, Japan*
[6]*Nagasaki University, 1-12-4 Sakamoto, Nagasaki, Nagasaki 852-8523, Japan*
[†]*Deceased*

Correspondence should be addressed to Keiko Ogami-Takamura; keiko.ogami@nagasaki-u.ac.jp

Received 13 September 2021; Revised 29 October 2021; Accepted 2 November 2021; Published 17 November 2021

Academic Editor: Paul Harrison

The human skeleton of a young adult male with marked asymmetry of the bilateral upper extremities was excavated from the Mashiki-Azamabaru site (3000–2000 BCE) on the main island of Okinawa in the southwestern archipelago of Japan. The skeleton was buried alone in a corner of the cemetery. In this study, morphological and radiographic observations were made on this skeleton, and the pathogenesis of the bone growth disorder observed in the left upper limb was discussed. The maximum diameter of the midshaft of the humerus was 13.8 mm on the left and 21.2 mm on the right. The long bones comprising the left upper extremity lost the structure of the muscle attachments except for the deltoid tubercle of the humerus. The bone morphology of the right upper extremity and the bilateral lower extremities was maintained and was close to the mean value of females from the Ohtomo site in northwestern Kyushu, Japan, during the Yayoi period. It is assumed that the anomalous bone morphology confined to the left upper extremity was secondary to the prolonged loss of function of the muscles attached to left extremity bones. In this case, birth palsy, brachial plexus injury in childhood, and acute grey matter myelitis were diagnosed. It was suggested that this person had survived into young adulthood with severe paralysis of the left upper extremity due to injury or disease at an early age.

1. Introduction

The presence of continuous external mechanical stimulation is essential for the maintenance of bone morphology and strength [1, 2]. Persistent paralysis of the motor nerves leads to paralysis of the corresponding muscles and restriction of bone and joint movement. This leads to a decrease in bone strength and subsequent changes in bone morphology. In this study, we present a clinical and social differential diagnosis of a male human skeleton (Mashiki 15) with marked asymmetry of both upper extremities, excavated from the Mashiki-Azamabaru site on the main island of Okinawa, in the southwestern archipelago of Japan in East Asia. According to the archaeological findings, it is considered that the site was constructed in the period 3000–2000 BCE. In the field of palaeopathology, there are not many reports of cases of bilateral asymmetry confined to the upper extremities. It would be of great palaeopathological value to discuss the significant bone asymmetry confined to the upper extremities observed in this case.

2. Materials and Methods

The Japanese archipelago is located east of the Asian continent and extends for about 3,500 km in a long, narrow line from north to south. The Ryukyu Islands, to which Okinawa Island belongs, where the Mashiki-Azamabaru site is located, are at the southern end of the Japanese archipelago (Figure 1). This site was discovered in 1981 during the redevelopment of the Mashiki area of Ginowan, Okinawa Prefecture, Japan, and excavations were carried out from 1985 to 1989 [3]. The period of this site is the middle period of the prehistoric shell midden culture on Okinawa Island (3000–2000 BCE). This corresponds to the Late Jomon to early Yayoi periods in Japan. The site is located on a dune in an alluvial lowland 4 to 5 m above sea level, about 180 m from the coastline, and 58 human skeletal remains (51 adults and 7 nonadults) were excavated. Among these human skeletal remains, one human skeleton (Mashiki 15) was found to have significant upper extremity asymmetry, with the left side thinner than the right.

Mashiki 15, discussed in this research, was excavated from the west side of the collective graves and was buried supine and extended in the east-southeast head position (Figure 2). Mashiki 15 was buried alone in a hole-shaped grave, so it is not possible to be confused with other human skeletal remains. The remaining part of Mashiki 15 is shown in Figure 3. The skeletal remains of Mashiki 15 have been legally preserved at our laboratory, which was involved in the excavation project. We investigated Mashiki 15 in detail using standard macroscopic techniques in bioarchaeology [4]. The sex of Mashiki 15 was determined from the morphological features of the skull and pelvic bones. The age of Mashiki 15 was estimated to be young adult based on the degree of closure of the skull's sutures [5] and the degree of occlusion of the crown of the teeth [6]. The estimated height of Mashiki 15 was 165.4 cm by applying Pearson's formula [7] to the maximum length of the right radius, 243 mm. The asymmetry of the extremity bone measurements was examined using the method of Trinkaus et al. [8] and Lieverse et al. [9]: 100 × (maximum – minimum)/minimum. The measurements of Mashiki 15 were compared with the mean values of adult male and female bones and measurements of nonadults (two equivalent to a 9-year-old and one equivalent to a 10-year-old) excavated from the Ohtomo site (Karatsu, Saga Prefecture, Japan; early to mid-Yayoi period, 3000–2000 BCE) in northwestern Kyushu, Japan [10, 11].

Bilateral humerus, radius, and ulna were imaged with a clinical multislice computed tomography (CT) (Activision 16, Toshiba, Tokyo, Japan) (X tube volume/current = 120 kV/100 mA, 0.5 mm thickness). The clinical multislice CT belongs to the Graduate School of Biomedical Sciences, Nagasaki University. Based on the obtained DICOM data, the left and right horizontal morphologies were compared in horizontal cross-sectional images obtained at the mid-height of the radius and at the height of the distal quarter of the ulna. The left and right sides of the humerus, radius, and ulna were also compared on horizontal cross-sectional images obtained at the level of the minimum circumference of the diaphysis, measured grossly. All DICOM images were read by two physicians, including a board-certified specialist of the Japanese Orthopaedic Association.

3. Results

3.1. Skull. The skull remained with the cranial crown, the right side of the face, and the left side around the orbit. There is no pronounced asymmetry in the remaining parts (Figure 4). The maximum cranial length and breadth of the head were 176 mm and 135 mm, respectively, and the maximum cranial breadth was slightly smaller than those of human skeletal remains excavated from the Gushikawajima site (Shimajiri, Okinawa Prefecture, Japan), 173 mm and 145 mm, respectively, which are close to those of the period [12]. The cephalic index was 76.7, indicating mesocephalic. The supraocular height was 65 mm, and although the facial height index cannot be determined from the remaining portion, it suggests a low face. Based on the development of the mastoid process, the protrusion of the marginal tubercle, and the large width of the frontal process, it was assumed to be male. An osteoma was found in the remaining right external auditory canal (Figure 4). The coronal, sagittal, and lambda sutures of the skull were open on the inner and outer plates. The degree of occlusal wear on the crown surface was 1–2 degrees according to Broca's evaluation method [13] and D by Lovejoy's method of evaluation [6], which provided a basis for determining that Mashiki 15 was a young adult.

3.2. Lower Extremity. As shown in Figure 3, the distal articular end was missing, but the femur, tibia, and fibula diaphysis were well preserved (Figure 5(a)). The right and left iliacs and part of the sciatic bones were present in the pelvis (Figures 3 and 5(a)). The narrow angle of the bilateral greater sciatic notches provided the basis for determining that this skeleton was male [14].

3.3. Upper Extremity. The right carpals remained with the trapezium, trapezoid, scaphoid, capitate, lunate, and triquetrum. Of the right phalanges, all the metacarpals and proximal phalanges and part of the middle phalanges remained. The left carpals and phalanges were not retained. The long bones of the upper extremity remained, the right and left humeri, radius, and ulna. The proximal articular end of the right humerus and the distal articular end of the right ulna were absent. The left humerus, ulna, and radius were absent at both articular ends. The transverse and circumferential diameters of all long bones of the left upper extremity were smaller than those of the right side (Figure 5(b), Table 1).

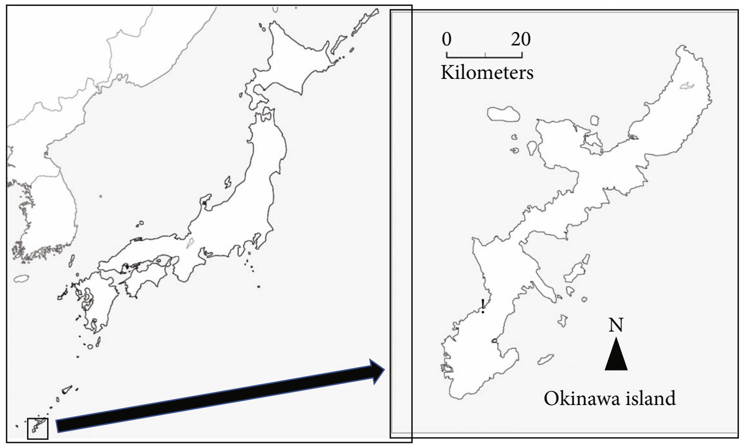

Figure 1: The Mashiki-Azamabaru site located in Ginowan, Okinawa Prefecture, Japan.

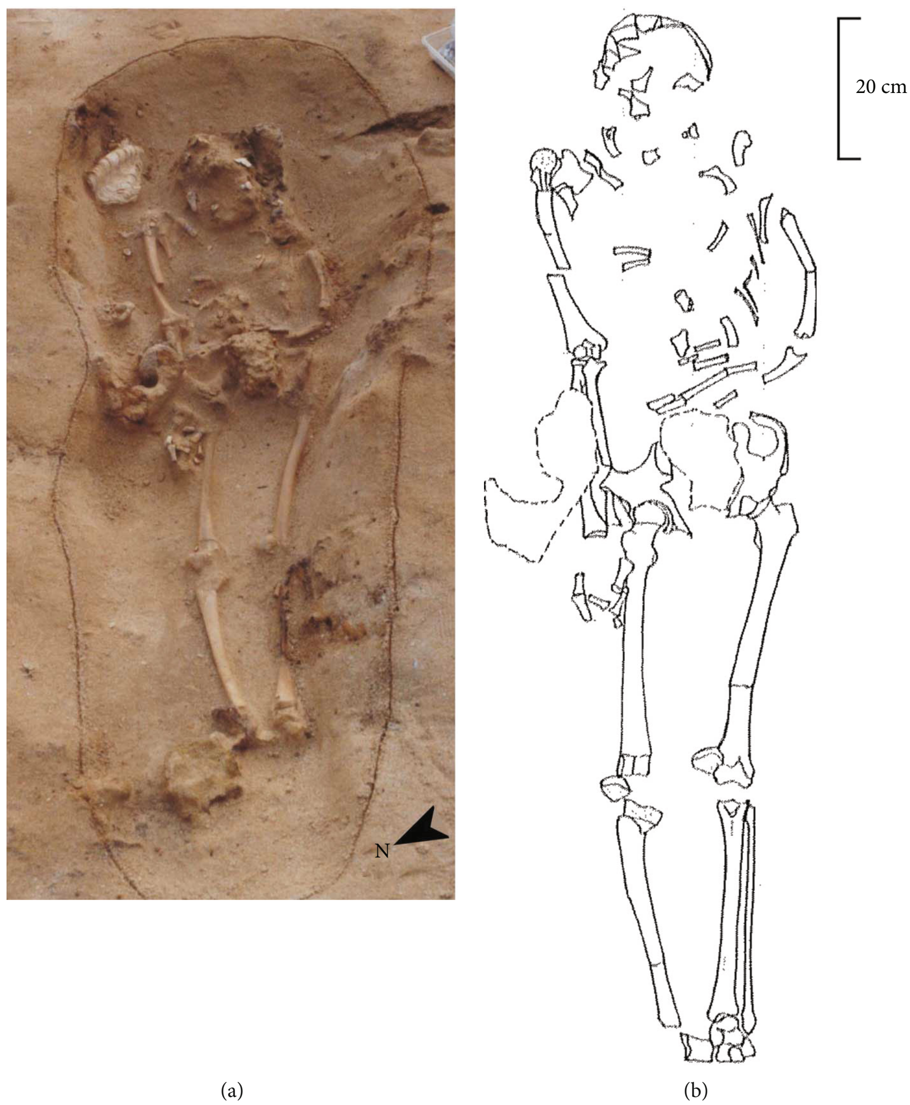

Figure 2: (a) Photograph of Mashiki 15, a young adult human skeleton buried alone in the Mashiki-Azamabaru site. (b) Schematic diagram of the skeletal remains of Mashiki 15 in its buried condition. There was no artificiality in the continuity and layout of the excavated skeleton.

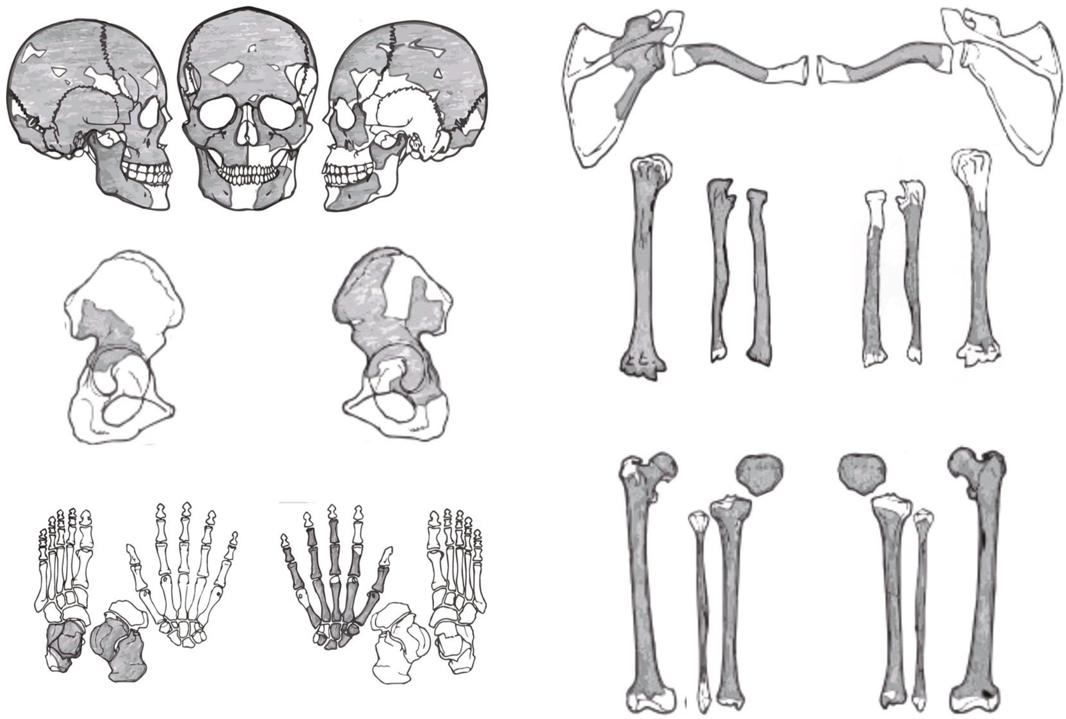

Figure 3: The remaining part of Mashiki 15. The shaded area is the residual part.

Figure 4: Anterior and right lateral views of the skull. The black arrow indicates the osteoma on the right external auditory canal.

The percentage asymmetry of the humerus was 53.6% for maximum diameter of the midshaft (Martin number; M5), 31.7% for minimum diameter of midshaft (M6), and 40.5% for the least circumference of the shaft (M7). In the radius, the maximum transverse shaft diameter (M4) was 27.0%, minimum sagittal shaft diameter (M5) was 46.6%, and minimum circumference (M3) was 35.7%. In the ulna, the dorsoventral shaft diameter (M11) was 60.7%, transverse shaft diameter (M12) was 75.8%, and least circumference (M3) was 46.2% (Table 1).

The length of the long bones of the left upper extremity was estimated from the remaining parts. The growth in the long axial direction was considered relatively normal. In the long bones of the left upper extremity, the features characteristic of muscle insertion, such as tubercles, tuberosity, crest, and grooves, were almost absent except for the deltoid tuberosity of the humerus (Figure 6(a)). In addition, the diaphyses were thin and had lost their biomechanical structure due to significant inhibition of their diaphyseal maturation. The right radius was preserved to the epiphysis, and this maximum length of 243 mm was applied to Pearson's formula to obtain an estimated height of 162.8 cm. This height is higher than the mean height of 156.8 cm for the male human remains examined at the Gushikawajima site

(a) (b)

Figure 5: (a) Comparison of both lower extremity bones. (b) Comparison of both upper extremity bones.

Table 1: Measurements of upper and lower extremity bones belonging to Mashiki 15 and percentage asymmetry calculated as 100 × (maximum − minimum)/minimum. Martin numbers are given in parenthesis as appropriate.

	Left (mm)	Right (mm)	Percentage asymmetry
Humerus			
Maximum diameter of midshaft (M5)	13.8	21.2	53.6
Minimum diameter of midshaft (M6)	12	15.8	31.7
Least circumference of the shaft (M7)	42	59	40.5
Radius			
Maximum transverse shaft diameter (M4)	11.5	14.6	27.0
Minimum sagittal shaft diameter (M5)	7.3	10.7	46.6
Minimum circumference (M3)	28	38	35.7
Ulna			
Dorsoventral shaft diameter (M11)	8.4	13.5	60.7
Transverse shaft diameter (M12)	9.1	16	75.8
Least circumference (M3)	26	38	46.2
Femur			
Anterior-posterior diameter of the midshaft (M6)	25.4	24.9	2.0
Mediolateral diameter of the midshaft (M7)	20.0	20.5	2.5
Circumference of the midshaft (M8)	74	73	1.4
Tibia			
Sagittal diameter at the midshaft (M8)	26.2	26.5	1.2
Transverse diameter at the midshaft (M9)	18.7	19.3	3.2
Circumference of the midshaft (M10)	71	73	2.8

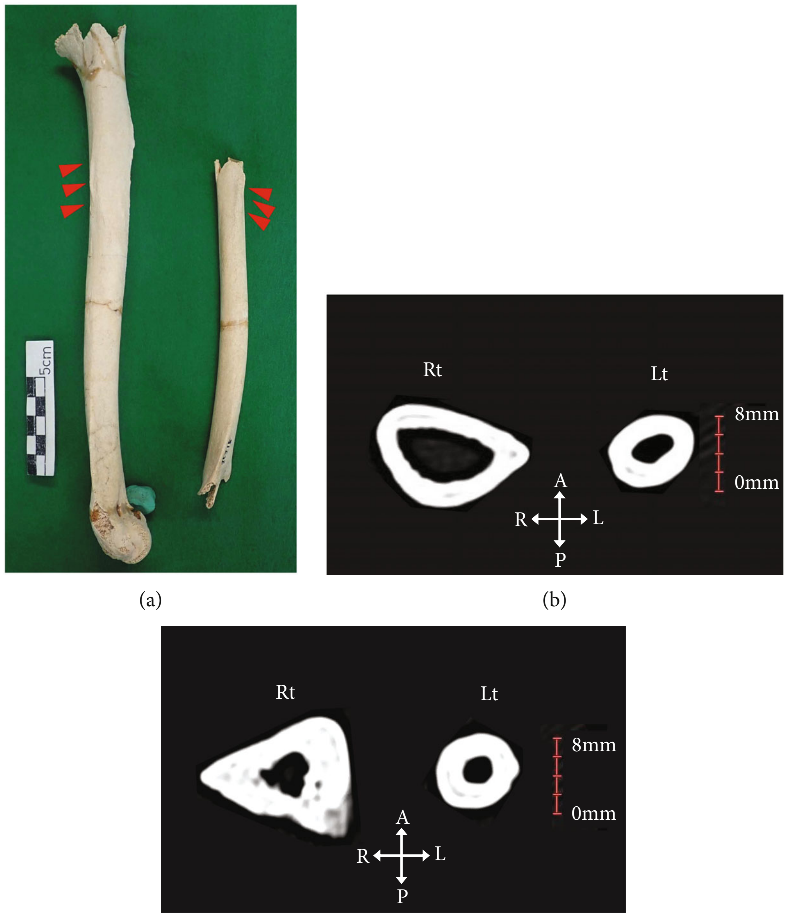

Figure 6: (a) Arrows indicate the deltoid tubercles of the bilateral humerus. (b) Cross-sectional images at the level of the distal quarter of the bilateral radius. (c) Cross-sectional images at the level of the middle of the bilateral ulna. A: anterior; P: posterior; R: right; L: left.

[12] in the Late Jomon period, which is geographically close to the Mashiki-Azamabaru site. As shown in Table 2, the measurements of the left humerus, radius, and ulna of Mashiki 15 were closer to those of a 9-year-old equivalent child than the means of adult males and females at the Ohtomo site [11]. The bone measurements of the right upper extremity of Mashiki 15 were closer to the means of the Ohtomo females [10].

As shown in Table 1, the overall transverse size of the humerus was significantly smaller on the left side. In the radius, the left radial tuberosity was lost post mortem. Therefore, it was not possible to identify any difference between the left and right sides at the articular end. In the radius diaphysis, the interosseous border of the left radius was slightly undeveloped compared to that of the right side (Figure 6(b)).

The left tuberosity of the ulna and the supinator crest were weakly developed and smooth. The interosseous border and posterior border were not well developed. The formation of the interosseous and posterior borders was significantly weaker than the right (Figure 6(c)).

The lateral portion of the clavicle remained on both sides. Although the left side was slightly narrower, there was no difference between the other upper extremity bones.

3.4. Computed Tomography Images. Cross-sectional CT images of the left and right humeri, ulna, and radius at the height of the minimum circumference measurement are shown (Figures 7(a)–7(c)). The shapes of the cross-sections of the diaphysis of the humerus, radius, and ulna were distorted and circular. The left and right sides were compared in a slice where the minimum circumference was measured. Although it is difficult to quantitatively assess the cortical bone due to artefacts and defects, a comparison of the images showed cortical bone thinning in the humerus and ulna on the left side compared to the right side. No thinning of the cortical bone was observed for the radius, but the interosseous margin was dulled.

4. Discussion

4.1. The Process of Bone Morphology Changes of Left Upper Extremity Bones. Generally, the muscles and bones of the dominant hand are more developed than those of the contralateral upper extremity, and the bony prominences at the muscle stops are also more developed [15, 16]. The background to this recognition is that the presence of continuous external mechanical stimulation is essential for maintaining bone morphology and strength [1, 2]. Therefore, when

Table 2: Comparison of the Mashiki 15 left-side humerus, radius, ulna, femur, and tibia measurements to the adult mean value dimensions and those of children of the Ohtomo site. Martin numbers are given in parenthesis as appropriate.

	Mashiki 15		Ohtomo site								
			Male, left			Female, left			9-year-old	9-year-old	10-year-old
	Left	Right	Mean	SD	*N*	Mean	SD	*N*	Right	Right	Right
Humerus											
Maximum diameter of midshaft (M6)	13.8	21.2	23.44	1.54	34	20.95	1.7	20	14.3	15.5	16
Minimum diameter of midshaft (M7)	12	15.8	17.58	1.64	33	15.8	0.95	20	10.7	12.1	12.2
Least circumference of the shaft (M8)	42	59	64.52	3.33	33	57.58	2.77	19	39	44	44
Radius											
Maximum transverse shaft diameter (M5)	11.5	14.6	17.12	1.17	25	16.36	1.28	11	10.6	11.5	10.7
Minimum sagittal shaft diameter (M6)	7.3	10.7	12.36	0.81	25	11.18	0.4	11	7.5	8.4	7.9
Minimum circumference (M4)	28	38	44.67	2.15	15	40.44	2.88	9	28	30.5	29
Ulna											
Dorsoventral shaft diameter (M12)	8.4	13.5	15.04	0.92	26	12.83	1.27	11	7.8	8.4	—
Transverse shaft diameter (M13)	9.1	16	17.15	1.38	26	15.91	1.12	12	11.1	11.9	—
Least circumference (M4)	26	38	37.18	2.9	22	33.86	1.35	7	—	25	—
Femur											
Anterior-posterior diameter of the midshaft (M7)	25.4	24.9	28.61	2.71	41	25.23	1.39	30	—	19.3	20.7
Mediolateral diameter of the midshaft (M8)	20	20.5	26.43	1.65	42	25.2	1.73	30	—	17	15.8
Circumference of the midshaft (M9)	74	73	86.98	5.46	41	80.41	4.46	29	—	57	58
Tibia											
Sagittal diameter at the midshaft (M9)	26.2	26.5	30.95	2.13	43	27.63	2.16	24	—	21.2	20.1
Transverse diameter at the midshaft (M10)	18.7	19.3	21.35	1.66	43	19.65	1.13	26	—	16.3	15.4
Circumference of the midshaft (M11)	71	73	83.39	5.56	41	75.26	4.4	23	—	50	57

permanent motor nerve paralysis results in muscle paralysis and restriction of bone and joint movement, bone strength is reduced, and subsequently, bone morphology is changed. Prolonged paralysis of the left upper extremity of Mashiki 15 caused muscle atrophy, leading to disuse atrophy. Disuse atrophy is a change that progresses over a period of years. Especially in the growing skeleton, the presence of motor paralysis leads to significant changes in bone morphology. Since the left upper extremity of Mashiki 15 was significantly thinner than the right upper extremity, it is assumed that the motor paralysis occurred at a younger age. Takeuchi [17] found that bone growth inhibition occurred in the transverse direction of membranous ossification in a patient who died after being bedridden for 16 years from birth due to hydrocephalus. However, there was minor retardation of growth in the longitudinal direction of cartilaginous ossification. The growth of all three extremities, except for the left upper extremity, was comparable to that of an adult female, indicating that Mashiki 15 was not bedridden and could maintain a certain amount of activity.

The paralysis of the muscles of the left upper extremity resulted in the loss of external mechanical stimulation and the suppression of membranous ossification of the bone. However, Mashiki 15 survived by carrying out some activities with the help of the upper extremity.

The preservation of the epiphyses is worse on the left side than on the right side of the upper extremity bones of Mashiki 15. Generally, the epiphyses contain more cancellous bone, which is less well preserved than the cortical bone of the diaphysis. Furthermore, in the present case, the left upper extremity bones were atrophic compared to the right, which could make the cancellous bones even more fragile. Thus, the difference in the preservation of the epiphyses between the right and left sides could be explained.

4.2. Differential Diagnosis of Mashiki 15. Neurological problems are the first suspected cause of motor paralysis of the extremities. In Mashiki 15, bone growth was observed in three extremities except for the left upper extremity, so systemic diseases like muscular dystrophy and congenital skeletal dysplasia were excluded from the differential diagnosis.

Paralytic diseases of the motor nerves can be broadly divided into central and peripheral paralyses. Central paralysis is caused by disorders of the brain or spinal cord, both of which are often severe enough to be life-threatening. The most common causes of paralysis due to brain damage are cerebral palsy, head trauma, cerebral infarction, and intracerebral haemorrhage. Paralysis due to spinal cord disease is caused by traumatic spinal cord injury or spinal cord tumours. Central paralysis often affects the lower extremities, and the complications are often severe [18, 19]. Given the level of medical care and living conditions in ancient times, it is assumed that those who suffered severe complications in childhood would have found it difficult to survive into adulthood. Because Mashiki 15 survived into young adulthood, the possibility of central nervous system paralysis is minimal.

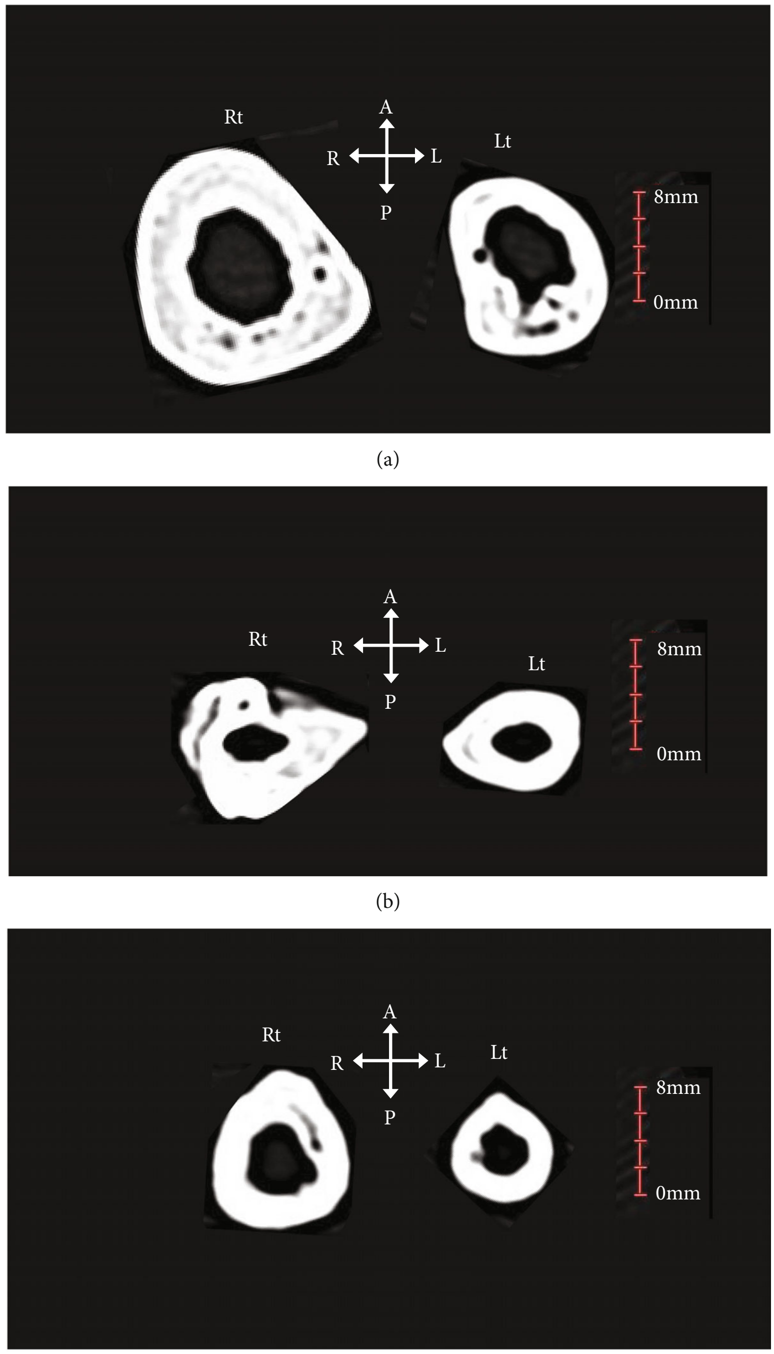

(a)

(b)

(c)

Figure 7: (a) Cross-sectional images of the bilateral humerus at the level of the minimum circumference measurement. (b) Cross-sectional images of the bilateral radius at the level of the minimum circumference measurement. (c) Cross-sectional images of the bilateral ulna at the level of the minimum circumference measurement. A: anterior; P: posterior; R: right; L: left.

Peripheral nerve palsy, on the other hand, is often limited in extent to the nerves that are paralysed and occurs in one side of the upper or lower extremity. Thus, it is possible to live a long life with some disabilities and limitations in daily life. Peripheral nerve palsy can be caused by various factors, including peripheral nerve damage from trauma, permanent compression of peripheral nerves from neoplastic disease, or infectious diseases such as acute poliomyelitis. Particularly in paralysis limited to one upper extremity, the differential includes brachial plexus injury due to trauma, delivery palsy at birth, and acute poliomyelitis due to polio.

The Brachial plexus comprises the fifth, sixth, seventh, and eighth cervical ventral rami and the first thoracic ventral ramus. It innervates the muscles, joints, and skin of the upper extremity. The brachial plexus travels from medial to lateral, dividing into the root, trunk, division, and cord, while branching nerves innervate various upper extremity parts [20].

Brachial plexus injury can be caused by external forces from high-energy trauma, such as a fall while riding a motorcycle or during high-speed sports such as skiing. It can also be damaged directly by a puncture wound in the supraclavicular fossa or a bone fragment from a clavicle fracture. Accidents resulting in high-energy trauma are unlikely to have occurred in the period when Mashiki 15 lived. However, the possibility of injury due to a fall from a height cannot be ruled out. The brachial plexus stretching can also injure it during delivery due to the force exerted by the birthing manoeuvre to separate the head from the shoulder. Brachial plexus palsy due to delivery is referred to as delivery palsy. Approximately 10–30% of infants who suffer brachial plexus injury at birth will have residual neurological deficits and will present with permanent changes in upper extremity development and function if not adequately treated [21].

Brachial plexus palsy is classified according to the height and extent of injury into superior (the fifth and sixth ± seventh cervical roots), total (the fifth to eighth cervical root + the first thoracic root), inferior (the eighth cervical and the first thoracic root), and intermediate (the seventh cervical root) types [22–25]. In all types, severe and permanent paralysis results in disuse atrophy of the musculoskeletal system of the upper extremities. The superior type presents with motor deficits in the upper arm from the shoulder to the elbow and sensory deficits in the proximal lateral upper arm and lateral forearm. The total type presents with motor and sensory deficits in the entire arm from the shoulder to the hand. The inferior type causes paralysis of the forearm and hand, but it is often considered the total type at the time of injury, followed by incomplete recovery of the superior nerve roots, resulting in the inferior type [26]. In Mashiki 15, the left deltoid tuberosity was developed, while the forearm diaphysis was remarkably slender, suggesting that the lower nerve roots were paralysed compared to the upper roots. In ancient times, there was no surgical treatment as we know it today for brachial plexus injury, so there was no choice but to let the injury heal naturally.

Acute poliomyelitis is a viral disease that usually occurs in childhood and is transmitted by faecal excretion of the virus, which enters the body orally [27]. In most cases, the infection is subclinical and lifelong immunity is acquired, but paralysis occurs in 0.1–0.2% of cases. Of these, only a small percentage become permanently paralysed [28]. Paralysis is most common in the lower extremities, with unilateral lower extremity monoplegia being the most common. It is followed by unilateral upper extremity, bilateral lower extremities, and facial muscles [29, 30]. Of the 58 human remains excavated from the Mashiki-Azamabaru site, only Mashiki 15 showed pathological asymmetry of the extremity bones. Therefore, the possibility of a polio epidemic at this site is unknown. Ishida and Suzuki [31] reported on the morphology of modern human skeletons with disuse atrophy of the extremities caused by acute poliomyelitis in childhood. They found that the growth of the transverse diameter of the affected long bone was more inhibited than that of the long axis. In contrast, the bony development of the ligamentous attachments and epiphyses was relatively good. The degree of the longitudinal development of the left upper extremity of Mashiki 15 is unknown because the epiphyses did not remain. However, the possibility of polio cannot be ruled out because of the characteristic of weak bony development at the muscle attachments.

Besides neurological problems, the differential diagnosis for this skeleton is disuse atrophy due to early childhood trauma. There are no obvious signs of fracture in the remaining skeleton of the left upper extremity, but it is still possible that there has been severe trauma to the nonremaining part of the body, especially to the proximal humerus. Fractures of the proximal humerus in patients who are skeletally immature or approaching skeletal maturity are rare, but it is now recognised that nonsurgical treatment generally leads to good functional results [32, 33]. On the other hand, given the level of medical care and the environment in ancient times, it is possible that the fracture could have not been treated appropriately, leading to disuse atrophy. However, even if there had been severe trauma to the proximal humerus as described, significant atrophy of the left upper extremity skeleton, as in the present case, could not be explained by this because the distal forearm and hand were still movable if the nerves were not damaged. Likewise, if there had been severe trauma to the nonremaining left elbow joint and hand in early childhood, it is unlikely that the entire left upper extremity skeleton would have atrophied as much as it did in this case. This is because if the injury is more distal, the proximal skeleton can move somewhat. This implies the presence of an external mechanical stimulus, which should be able to maintain the morphology and strength of the skeleton.

4.3. Palaeopathological Reports of Bone Growth Disorder in the Unilateral Upper Extremity. There are several palaeopathological reports about the growth of unilateral upper extremity bones. Hershkovitz et al. [34] reported a right-side dominant asymmetry in a male human skeleton, Ohalo II, excavated from the Upper Palaeolithic Ohalo site in Israel and diagnosed it as an adult-onset Erb-Duchenne-type brachial plexus palsy of the left upper extremity. On the other hand, Trinkaus [35] reexamined Ohalo II based on a comparison with data from other human skeletons from the Upper Palaeolithic. Based on this comparison, it was concluded that the asymmetry of the upper extremity bones of Ohalo II was within the expected range for Upper Palaeolithic human remains and that there is no evidence for an upper extremity anomaly. Churchill and Formicola [36] reported bilateral differences in the upper extremity bones of an adult male skeleton labelled Barma Grande 2, excavated from an Upper Palaeolithic cave in Barzilossi, Liguria, Italy. The percentage asymmetry calculated for Barma Grande 2 as $100 \times (\text{right} - \text{left})/\text{left}$ was smaller than that for Mashiki 15. The authors suggest that the factors that produced the asymmetry in Barma Grande 2 developed after the skeleton had matured, as the asymmetry in the diaphysis was greater than that in the articular and muscular insertions.

Lieverse et al. [9] reported an adult male skeleton with severe bilateral upper extremity asymmetry, designated

Shamanka II 29.1, from the early Neolithic cemetery of Shamanka II on the south coast of Lake Baikal, Siberia, Russia. The most striking asymmetry was between the bilateral humerus, ranging from 11.7% to 89.5%. In the diseased extremity, no structures of muscle attachment, including the deltoid tuberosity, were observed. Because the asymmetry extended over the entire upper extremity, the authors concluded that it reflected complete brachial palsy occurring before the arm skeleton matured. In the skeleton of Mashiki 15, the greatest degree of asymmetry was observed in the bilateral ulna, with a range of 46.2% to 75.8%. The presence of the left deltoid tubercle of Mashiki 15, which was absent in Shamanka II, suggests that the brachial plexus injury was not the complete total type but rather a pathology with incomplete recovery of at least the fifth cervical root from the total type.

5. Conclusion

Mashiki 15, a human skeleton from the middle to late Okinawa Shell Midden Period, was buried alone at the Mashiki-Azamabaru site in Okinawa Prefecture. The most likely disease of this asymmetry was the brachial plexus palsy, which was considered to have been caused by birth palsy, trauma, or acute poliomyelitis in childhood. The type of brachial plexus injury was not the total type, as the deltoid tubercle was observed, and it was assumed that the fifth cervical root was not originally injured or that it had recovered incompletely from the total type. Prolonged motor nerve paralysis results in disruption of the skeletal remodelling process, leading to impaired bone growth. Any paralytic disease would have taken years or longer to produce changes in bone tissue. Even in ancient times, when the medical and welfare environment was not as well developed as it is today, there was a strong fellowship and a mentally stable society that accepted the existence of individuals with long-term physical disabilities, such as in this case. The palaeopathological study of Mashiki 15 would provide an essential basis for the future interpretation and diagnosis of similar cases.

Data Availability

The data used to support the findings of this study are included in the article.

Conflicts of Interest

The authors declare that there is no conflict of interest regarding the publication of this paper.

References

[1] J. Wolff, *The Law of Bone Remodelling*, Springer, New York, 1986.

[2] C. T. Rubin and L. E. Lanyon, “Osteoregulatory nature of mechanical stimuli: function as a determinant for adaptive remodeling in bone,” *Journal of Orthopaedic Research*, vol. 5, no. 2, pp. 300–310, 1987.

[3] T. Shinzato, “Prehistoric burial customs in the Ryukyu archipelago (3): the Okinawa Islands,” *Journal of the Doctorate Studies in Social Sciences*, vol. 8, pp. 101–127, 2011.

[4] R. Martin and R. Knussmann, *Anthropologie Band I*, Gustav Fischer Verlag, Stuttgart, 1988.

[5] C. Masset, “Age estimation on the basis of cranial sutures,” in *Age Markers in the Human Skeleton*, M. Y. Işcan, Ed., pp. 71–103, Thomas CC, Springfield, 1989.

[6] C. O. Lovejoy, R. S. Meindl, R. P. Mensforth, and T. J. Barton, “Multifactorial determination of skeletal age at death: a method and blind tests of its accuracy,” *American Journal of Physical Anthropology*, vol. 68, no. 1, pp. 1–14, 1985.

[7] K. Pearson, “IV. Mathematical contributions to the theory of evolution.—V. On the reconstruction of the stature of prehistoric races,” *Philosophical Transactions of the Royal Society of London*, vol. 192, pp. 169–244, 1899.

[8] E. Trinkaus, S. E. Churchill, and C. B. Ruff, “Postcranial robusticity inHomo. II: humeral bilateral asymmetry and bone plasticity,” *American Journal of Physical Anthropology*, vol. 93, no. 1, pp. 1–34, 1994.

[9] A. R. Lieverse, M. A. Metcalf, V. I. Bazaliiskii, and A. W. Weber, “Pronounced bilateral asymmetry of the complete upper extremity: a case from the early Neolithic Baikal, Siberia,” *International Journal of Osteoarchaeology*, vol. 18, no. 3, pp. 219–239, 2008.

[10] S. Isotani, S. Noriyasu, M. Nagai, and Y. Naito, “Human skeletal remains from the Yayoi period excavated at the Ohtomo site, Saga prefecture,” *Ohtomo site Reprint*, pp. 1–48, 1981.

[11] T. Wakebe, “Nonadult skeletal remains excavated from the Ohtomo site, Saga prefecture,” *Ohtomo site Reprint*, pp. 1–11, 1981.

[12] N. Doi, “Human skeletal remains from Gushikawajima island sites,” *Research Report of Okinawa Prefectural Archaeological Center*, vol. 64, pp. 245–260, 2012.

[13] J. J. Pindborg, “Chronic mechanical injuries,” in *Pathology of the Dental Hard Tissues*, J. J. Pindborg, Ed., pp. 294–311, Munksgaard, Copenhagen, 1970.

[14] D. H. Ubelaker, *Human Skeletal Remains: Excavation, Analysis, Interpretation*, Taraxacum, Washington, 1989.

[15] A. Blackburn and C. J. Knüsel, “Hand dominance and bilateral asymmetry of the epicondylar breadth of the Humerus,” *Current Anthropology*, vol. 47, no. 2, pp. 377–382, 2006.

[16] K. G. Zelazny, A. D. Sylvester, and C. B. Ruff, “Bilateral asymmetry and developmental plasticity of the humerus in modern humans,” *American Journal of Physical Anthropology*, vol. 174, no. 3, pp. 418–433, 2021.

[17] S. Takeuchi, “A case of growth transformation in unexercised limb bones,” *Journal of the Anthropological Society of Nippon*, vol. 99, no. 3, pp. 319–332, 1991.

[18] N. Bass, “Cerebral palsy and neurodegenerative disease,” *Current Opinion in Pediatrics*, vol. 11, no. 6, pp. 504–507, 1999.

[19] K. W. Krigger, “Cerebral palsy: an overview,” *American Family Physician*, vol. 73, no. 1, pp. 91–100, 2006.

[20] A. Ross, “Pectoral girdle and upper limb: overview and surface anatomy,” in *Gray's Anatomy: The Anatomical Basis of Clinical Practice*, S. Standring, Ed., pp. 871–940, Elsevier, Philadelphia, 2021.

[21] W. Pondaag, M. J. Malessy, J. Gert van Dijk, and R. T. Thomeer, “Natural history of obstetric brachial plexus palsy: a systematic review,” *Developmental Medicine and Child Neurology*, vol. 46, no. 2, pp. 138–144, 2004.

[22] P. C. Brunelli, D. Robecchi, and L. Lenzi, "Computerized axial tomography in obstetrical paralysis of the brachial plexus," *Italian Journal of Orthopaedics and Traumatology*, vol. 12, no. 4, pp. 507–514, 1986.

[23] R. S. Boome and J. C. Kaye, "Obstetric traction injuries of the brachial plexus. Natural history, indications for surgical repair and results," *The Journal of Bone and Joint Surgery British volume*, vol. 70-B, no. 4, pp. 571–576, 1988.

[24] M. M. Al-Qattan, H. M. Clarke, and C. G. Curtis, "Klumpke's birth Palsy," *Journal of Hand Surgery*, vol. 20, no. 1, pp. 19–23, 1995.

[25] K. L. Buterbaugh and A. S. Shah, "The natural history and management of brachial plexus birth palsy," *Current Reviews in Musculoskeletal Medicine*, vol. 9, no. 4, pp. 418–426, 2016.

[26] A. H. Jahnke Jr., D. F. Bovill, H. R. McCarroll Jr., P. James, and R. K. Ashley, "Persistent brachial plexus birth palsies," *Journal of Pediatric Orthopedics*, vol. 11, no. 4, pp. 533–537, 1991.

[27] D. Kidd, A. J. Williams, and R. S. Howard, "Poliomyelitis," *Postgraduate Medical Journal*, vol. 72, no. 853, pp. 641–647, 1996.

[28] D. T. Jamison, A. M. Torres, L. C. Chen, and J. L. Melnick, "Poliomyelitis: what are the prospects for eradication and rehabilitation?," *Health Policy and Planning*, vol. 6, no. 2, pp. 107–118, 1991.

[29] D. O. Wiechers, "Acute and latent effect of poliomyelitis on the motor unit as revealed by electromyography," *Orthopedics*, vol. 8, no. 7, pp. 870–872, 1985.

[30] G. R. Young, "Occupational therapy and the postpolio syndrome," *The American Journal of Occupational Therapy*, vol. 43, no. 2, pp. 97–103, 1989.

[31] H. Ishida and T. Suzuki, "An osteological study of disused atrophic bones after childhood poliomyelitis," *Journal of the Anthropological Society of Nippon*, vol. 93, no. 4, pp. 447–460, 1985.

[32] E. C. King and S. B. Ihnow, "Which proximal humerus fractures should be pinned? Treatment in skeletally immature patients," *Journal of Pediatric Orthopedics*, vol. 36, Supplement 1, pp. S44–S48, 2016.

[33] R. Shahriar and P. Hosseinzadeh, "Proximal humerus fractures: what alignment is acceptable in children 10 and up?," *Journal of Pediatric Orthopedics*, vol. 41, Supplement 1, pp. S20–S23, 2021.

[34] I. Hershkovitz, G. Edelson, M. Spiers, B. Arensburg, D. Nadel, and B. Levi, "Ohalo II man—unusual findings in the anterior rib cage and shoulder girdle of a 19000-year-old specimen," *International Journal of Osteoarchaeology*, vol. 3, no. 3, pp. 177–188, 1993.

[35] E. Trinkaus, "The palaeopathology of the Ohalo 2 upper paleolithic human remains: a reassessment of its appendicular robusticity, humeral asymmetry, shoulder degenerations, and costal lesion," *International Journal of Osteoarchaeology*, vol. 28, no. 2, pp. 143–152, 2018.

[36] S. E. Churchill and V. Formicola, "A case of marked bilateral asymmetry in the upper limbs of an upper palaeolithic male from Barma Grande (Liguria), Italy," *International Journal of Osteoarchaeology*, vol. 7, no. 1, pp. 18–38, 1997.